Aalto University
School of Chemical
Technology

School of Chemical Technology

Degree Programme of Materials Science and Engineering

Outi Järvinen

HYDROMETALLURGICAL REMOVAL OF ZINC FROM STAINLESS STEEL FLUE DUSTS

Master's thesis for the degree of Master of Science in Technology submitted for inspection, Espoo, 2 August, 2013.

Supervisor **Docent Jari Aromaa**

Instructor **M.Sc. Antti Kekki**

Aalto University
School of Chemical
Technology

Aalto University, P.O. BOX 11000, 00076 AALTO
www.aalto.fi

Abstract of master's thesis

Author Outi Järvinen		
Title of thesis Hydrometallurgical removal of zinc from stainless steel flue dusts		
Department Material Science and Engineering		
Professorship Corrosion and hydrometallurgy	**Code of professorship** MT-85	
Thesis supervisor Docent Jari Aromaa		
Thesis advisor M.Sc. (Tech) Antti Kekki		
Date 31.7.2013	**Number of pages** 72+10	**Language** English

Abstract

Stainless steel flue dusts are problematic to the steel industry because of their chemical composition that makes direct recycling and landfilling impossible. Pyrometallurgical and hydrometallurgical processes have been tested in dust treatment. At the moment, most of the processes that have reached commercialization have been pyrometallurgical. Still, it is thought that hydrometallurgy could offer solutions especially in small scale on-site treatment as it is less energy intensive and requires a smaller investment than pyrometallurgical processes.

In the theoretical part of this work, the problematic related to flue dusts is considered and some of the tested treatment processes are described. One chapter in this part deals with relevant hydrometallurgical principles and outlines the most recent research in the field of sulfuric acid leaching

The experimental part of the work introduces a multi-phase process that was tested for removing zinc from five different stainless steel dust samples (CRK, VKU1, VKU2, AOD1 and AOD2). The process consisted of three phases: water washing, leaching with 0,5 M sulfuric acid and leaching with alternatively 2 M or 6 M sulfuric acid.

Results from the experiments lead to conclude that a multi-phase leaching process might not offer the desired benefits in zinc removal. Highest zinc removal rates were observed when the second leaching step was carried out in 2 M acid; CRK 62%, VKU1 58 %, VKU2 50 %, AOD1 61 % and AOD2 59 %).

The leaching of alloying elements Cr, Ni and Mo was also monitored during the process. Cr and Ni were found to be less soluble than Mo, which was leached already in the first step of the process chain. Additionally, the water washing step on the other hand was found to be efficient in removing chlorides from the dusts.

Keywords stainless steel, flue dusts, zinc, H_2SO_4, acid leaching

Aalto-yliopisto
Kemian tekniikan
korkeakoulu

Aalto-yliopisto, PL 11000, 00076 AALTO
www.aalto.fi

Diplomityön tiivistelmä

Tekijä Outi Järvinen		
Työn nimi Hydrometallurgical removal of zinc from stainless steel flue dusts		
Laitos Materiaalitekniikan laitos		
Professuuri Korroosio ja hydrometallurgia		**Professuurikoodi** MT-85
Työn valvoja Dosentti Jari Aromaa		
Työn ohjaaja DI Antti Kekki		
Päivämäärä 31.7.2013	**Sivumäärä** 72+10	**Kieli** Englanti

Tiivistelmä

Tuotantoprosessin aikana syntyvät lentopölyt aiheuttavat ongelmia terästeollisuudelle. Niiden suora kierrätys tai läjitys kaatopaikalle on kemiallisen koostumuksen takia mahdotonta. Sekä pyro – että hydrometallurgisia menetelmiä on tutkittu pölyjen käsittelemisessä, mutta täysin tyydyttävää prosessia ei ole vielä tällä hetkellä olemassa. Enemmistö kaupallistetuista käsittelyprosesseista on perustunut pyrometallurgisiin menetelmiin. Hydrometallurgisten prossien on kuitenkin ajateltu tarjoavan uusia mahdollisuuksia etenkin pienien pölymäärien käsittelyssä.

Työn teoreettisessa osassa käsitellään lentopölyihin liittyviä ongelmia ja esitellään joitakin tärkeimpiä käsittely menetelmiä. Hydrometallurgian teoriaa, ja viimeisintä rikkihappoliuotukseen liittyvää tutkimustietoa käsitellään omissa luvuissaan.

Työn kokeellisessa osassa esitellään työn aikana testattu monivaiheinen liuotusprosessi, jonka tarkoituksena oli sinkin liuottaminen viidestä eri pölynäytteestä (CRK, VKU1, VKU2, AOD1 and AOD2). Testattu prosessi koostui kolmesta vaiheesta: vesipesu, liuotus 0,5 M rikkihapolla, ja liuotus vaihtoehtoisesti 2 M tai 6 M rikkihapolla.

Kokeista saatujen tulosten perusteella monivaiheinen liuotusprosessi ei näytä tuovan erityistä lisäarvoa sinkin liuottamiseen. Sinkki liukeni pölyistä parhaiten 2 M rikkihapossa, jollin sato prosentit olivat seuraavat: CRK 62 %, VKU1 58 %, VKU2 50 %, AOD1 61 % and AOD2 59 %.

Tutkimuksessa tarkasteltiin myös kromin, nikkelin ja molybdeenin liukenemista prosessin aikana. Kromin ja nikkelin havaittiin olevan vaikeammin liuotettavissa kuin molybdeenin, joka liukeni jo prosessin ensimmäisessä vaiheessa. Työssä havaittiin myös, että vesipesu on tehokas tapa kloridien poistamiseen pölyistä.

Avainsanat ruostumaton teräs, lentopöly, sinkki, happoliuotus, H_2SO_4

FOREWORD

This thesis was done 1.2.2013 – 31.7.2013 in the Research Group of Corrosion and Hydrometallurgy in Aalto University. The thesis is part of the Tekes funded FIMECC-METDUST research project that focuses on investigating new hydrometallurgical solutions for steel mill ferrous dust and sludge treatment.

I would like to thank Professor Olof Forsén for the interesting topic and especially for the opportunity to work as a part of the research group. My supervisor Docent Jari Aromaa and my instructor M.Sc. (Tech) Antti Kekki, I want to thank for support during the thesis and for sharing their extensive knowledge on the research topic. Discussions and weekly meetings with them were immensely valuable.

Special thanks go additionally to Istvan Gaffi for his help with practical laboratory work, and for the whole research group for creating a supportive working atmosphere.

At last I would like to thank my family for always being there for me during my studies and the making of this there.

Espoo, 31st July, 2013

Outi Järvinen

Table of Contents

1 INTRODUCTION

Flue dusts are generated in rather large amounts during stainless steel production and they are problematic to the industry for several reasons. Firstly, because of their chemical composition, they cannot be directly recycled back to the steelmaking process nor used as raw material in the production of other metals or landfilled. The dusts contain elements that cause problems in further processing as well as elements that are environmentally harmful. Secondly, if the dust cannot be treated and recycled, valuable potential raw material will be lost.

In general, the majority of problems in recycling are caused by accumulation of zinc to the flue dusts. Zinc is one of the primary elements in the dusts because of the usage of galvanized steel scrap as raw material. It is present as easily soluble zincite (ZnO) or refractory franklinite ($ZnFe_2O_4$), which is a spinel group mineral. Other problematic elements in the dusts include halides and heavy metals such as lead and cadmium. Heavy metal content makes landfilling regulated while halides are detrimental to zinc electrolysis. There has been plenty of research on alternative ways to remove zinc from the dusts in the form of compounds that could be further used in zinc production [Caravaca *et al.* 1994, Cruelles *et al.* 1992, Denton 2005, Dutra 2006, Goff *et al.* 2004, Havlik *et al.* 2006, Herlitz 1982, Herrero *et al.* 2010, Hoang Trung *et al.* 2011, Kekki *et al.* 2011 & 2012, Kelebek *et al.* 2004, Kemperman 2010, Langova *et al.* 2007, Leclerc *et al.* 2003, Maccagni *et al.* 2010, Majuste *et al.* 2008, Nakamura *et al.* 2008, Oustadakis *et al.* 2010, Palencia *et al.* 1999, Stefanova *et al.* 2012 & 2013, Reyad 2010, Xia *et al.* 2000]. Research has mostly concentrated on carbon steel dusts whereas only a few papers have investigated zinc removal from stainless steel dusts [Denton 2005, Goff *et al.* 2004, Kekki *et al.* 2011 & 2012, Majuste *et al.* 2008, Stefanova *et al.* 2012 & 2013]. Both pyrometallurgical and hydrometallurgical processes as well as hybrid processes have been tested but an entirely satisfying process doesn't really exist at the moment [Zunkel 2001, Nakamura *et al.* 2008, Xia *et al.* 2000].

The dusts that were studied in this thesis originated from a stainless steel plant, and besides iron and zinc they contained chromium, nickel and molybdenum. The purpose of this thesis was to investigate the leaching of zinc, concentrating especially in breaking the refractory franklinite structure by a multistage leaching process. Leaching

behavior of other elements was also monitored, focusing especially on valuable alloys nickel, molybdenum and chromium. Additionally, a pre-treatment for halide removal was investigated.

Three research questions were formulated from the previous objectives:

1. Can a multistage leaching process be used in breaking franklinite and can it enhance zinc removal from flue dusts?
2. How do Ni, Mo and Cr behave during the process?
3. Can halides be removed from the dusts by water washing pre-treatment?

In order to find answers to the research question, a three stage process was studied in detail. The process steps were designed to selectively leach specific compounds from the dusts and break different zinc containing mineral structures. The process steps are described below and the process is depicted by a flow chart in Figure 1.

i. Washing with distilled water in order to leach halides that are detrimental to zinc electrolysis.
ii. Leaching with dilute (0.5 M) sulfuric acid to leach zinc that is in oxide form (ZnO).
iii. Leaching alternatively with 2 M or 6 M sulfuric acid to leach zinc that is bound to refractory zinc ferrites ($ZnFe_2O_4$). Tests were done with both acid concentrations.

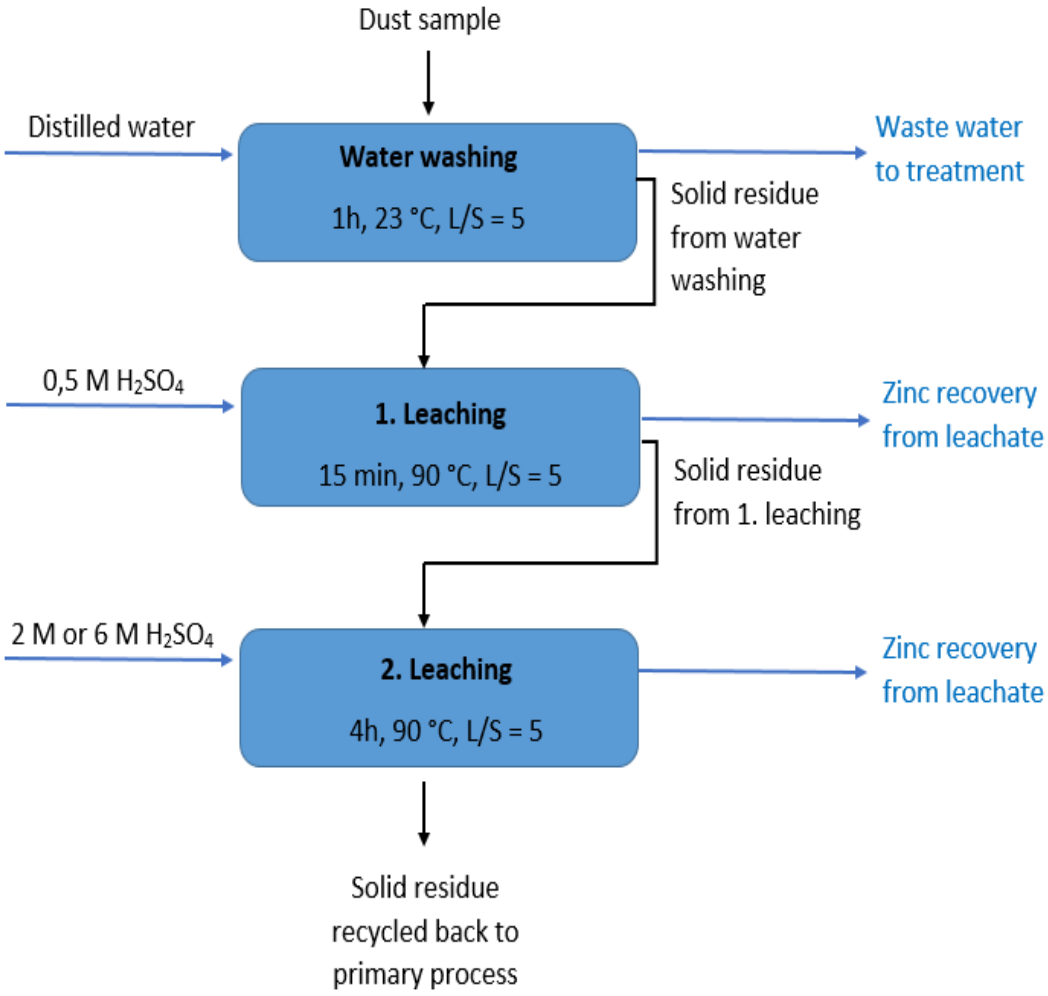

Figure 1. Flow chart of the tested multistage process.

2 STAINLESS STEEL FLUE DUSTS

This chapter introduces the formation mechanisms and general characteristics of stainless steel flue dusts. At the end of the chapter, problems arising from the composition of the dusts are discussed together with prospects in dust recycling and treatment.

2.1 Formation of dust particles

The core of the process chain for producing stainless steel is depicted in Figure 2. First, liquid ferrochrome is treated in the ferrochrome converter (Cr-converter) to lower its carbon content. Next, the converted ferrochrome is charged to the electric arc furnace (EAF) with recycled steel scrap and melted. The molten mixture is then decarburized in an argon oxygen decarburization converter (AOD) from which it is casted and can proceed to following process steps.

Figure 2. Stainless steel production process [Brink Helsinki Oy].

Nearly all flue dusts, a total of 30 to 70 kg per ton of produced stainless steel [Denton 2005, Goff *et al*. 2004, Zunkel 2001, Li *et al* 1992], come from the Cr-converter, EAF and AOD. Temperatures in Cr-converter, EAF and AOD can rise up to 1600 °C, where elements such as Fe, Zn, Pb and Cd are volatilized to the vapor phase. When the temperature of the vapor phase drops, vaporized material oxidizes and condenses generating new compounds, including ZnO and $ZnFe_2O_4$ [Machado *et al* 2006, Nyirenda 1991]. Zinc volatilization is especially due to higher vapor pressure compared with iron, and to the fact that zinc has very low solubility to molten slag [Laforest *et al*

2006, Machado *et al*. 2006, Oustadakis *et al.* 2010]. The fumes are extracted from the furnace through an opening in the roof and then pre-combusted and cleaned. Agglomeration of small dust particles takes place in the cooler parts of the off-gas system. The dust that is transported in the fumes is then collected in large bag filters in the bag house. Guézennec *et al.* [Guezennec *et al.* 2005] have comprehensively studied the formation mechanisms of dust particles in the EAF and identified five emission mechanisms (see also Figure 3):

1 Volatilization. Taking place in the arc zone (1) and the oxygen jet zone (1´) as well as in bursting of CO bubbles

2 Projection of droplets at the impact points of the arc (2) or oxygen jet (2`)

3 Bursting of CO bubbles coming from steel bath decarburization (3)

4 Bursting of droplets that are in contact with oxidizing atmosphere within the surface (4). Though this mechanism is uncertain in the EAF.

5 Direct fly-off of solid particles (5). Related to the introduction of powder materials into the furnace.

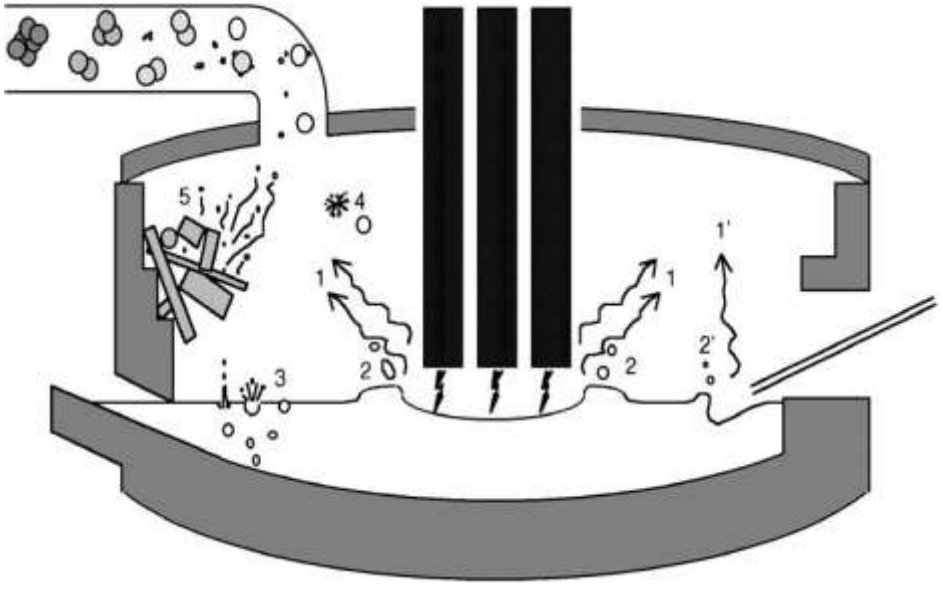

Figure 3. Dust formation mechanisms in the EAF [Guezennec *et al.*2005].

From these mechanisms, 1 and 3 actually account for almost 90 % of all dust formation. Direct volatilization and the bursting of CO bubbles account for 27 % and 60 % of the dust respectively. In the same study, it was also found out that CO bubble size is a key parameter in dust formation. By decreasing the bubble size, the amount of dust could be reduced. Critical bubble diameter was found out to be 4.5 mm; under that no film drops were formed at bubble burst. [Guezennec *et al.* 2005]. It is estimated that EAF generates around 10-25 kg of dust per ton of production [Laforest *et al.*2006, Majuste *et al.*2008, Rao 2006].

Because stainless steel making dusts have been less studied, there is not much information about the dust formation mechanisms in Cr- or AOD-converters. Ma *et al.* evaluate that some 3 % of all stainless steel dusts are formed in the AOD- converter, and that the prevailing formation mechanism is the bursting of gas bubbles during decarburization. Majuste *et al.* [Majuste *et al.* 2008] report that 20-30 kg of dust is created in the AOD per ton of stainless steel. In Cr-converters, dust is formed by the ejection and vaporization of metal and slag through electrode holes and by direct capturing of materials in the off-gas [Ma *et al.* 2006].

2.2 Chemical composition

Most of the research has been concentrated on carbon steel making flue dusts whereas only few articles have been written about stainless steel flue dusts [Majuste *et al.* 2008, Laforest *et al.* 2006]. Carbon steelmaking flue dusts have been quite extensively covered in literature and it is commonly observed that they have a complex chemical and mineralogical structure, which depends on the steel grade, the composition of the charge as well as the operating conditions of the process.

Stainless steel flue dusts have been studied much less, but they can be viewed as a sub-category of carbon steel flue dusts, having somewhat similar composition. Differences are brought on by greater usage of alloying elements and higher amounts of scrap as raw material. Stainless steel flue dusts have typically lower zinc content but are richer in Cr, Mo, Ni and Mn [Nyirenda 1991]. Some typical values for flue dusts from different sources are presented below in Table 1.

Table 1. Typical metal content (%) in different types of flue dusts [Meurer *et al.* 2001].

	Flue dusts with low zinc content		Flue dusts with high zinc content	Stainless steel flue dusts
	Blast Furnace	**BOF**	**EAF**	**EAF, AOD etc.**
Zn	0.1 - 5	1 - 10	15 - 40	2 - 4
Fe	25 - 35	55 - 65	25 -40	25 - 40
Cr	-	-	-	10 - 15
Mo	-	-	-	1 -2
Ni	-	-	-	3 - 5
Pb	0.05 - 1	0.5 – 1.5	2 - 6	0.5 - 1
Cu	0.01	0.01	0.1 – 0.3	0.2

The dusts main component is iron. Different studies report iron percentages between 15 and 62 %, the average being somewhere near 43 % [Laforest *et al.* 2006]. Zinc percentage in EAF steel making dusts can also vary significantly; values between 2-40 % are found in literature. In stainless steel dusts, zinc content is lower than in carbon steel dusts; only between 2-6 %.

Additionally, the dusts contain elements that originate from slag. These include compounds of calcium, potassium, magnesium and chloride. In stainless steel dusts, percentages of alloying elements like chromium, nickel and molybdenum are found to be between 10-15 %, 3-5% and 1-2%, respectively. [Meurer *et al.* 2001, Nyirienda 1991, Makkonen *et al.* 2010]

2.3 Mineralogy

Small particle size and overall complexity of the dust make precise mineralogical analysis challenging for typical analyzing methods XRD and SEM. The dusts are mainly a mixture of different metal oxides, sulfates and silicates [Sofilic *et al.* 2004], but each dust has to be examined individually to gain more exact information about its mineralogy.

Mineralogical phases that have been identified in different studies are presented in Table 2. When a dust treatment process is being designed, it especially important to pay attention to the occurrence of zinc that is predominantly present as zincite (ZnO) or

franklinite ($ZnFe_2O_4$). The proportion of franklinite is around 50 % of the total zinc content [Leclerc *et al.* 2006]. As pointed out earlier, ZnO is easily leached, while franklinite is very refractory and will only dissolve in strong acids.

Considering the valuable alloying elements, a leachability study by Laforest *et al.* [Laforest *et al.* 2006] reports that Cr and Ni were found to be tightly bound to iron or chromium oxides or spinel group minerals.

Table 2. Possible phases present in flue dusts [Havlik *et al.* 2010, Ma *et al.* 2006, Makkonen *et al.* 2010, Nyirienda 1991].

Element	Identified phases
Fe	Magnetite (Fe_3O_4), hematite (Fe_2O_3), zinc ferrite, chromite, metallic iron
Zn	Zincite (ZnO), zinc ferrite ($ZnFe_2O_4$), $ZnCl_2$, metallic zinc
Cr	Chromite ($FeCr_2O_4$), magnesio chromite $MgCr_2O_4$, CrO, replacing Fe in Fe_3O_4 spinel
Ni	NiO, replacing Fe in Fe_3O_4 spinel, metallic Ni
Mo	MoO, MoO_3
Pb	PbO, $PbCl_2$, $PbSO_4$, $PbCO_3$
Ca	Lime (CaO), $CaCO_3$, CaF_2, may also occur as ferrite or silicate
Si	Mainly as quartz (SiO_2)
Mg	Magnesioferrite ($MgFe_2O_4$), magnesiochromite ($MgCr_2O_4$), MgO
Halides (Cl, Na, F, K)	Present as salts or chlorides: NaCl, KCl, $ZnCl_2$

2.4 Particle size and morphology

The reported mean particle size of the dusts is very small; usually less than 10 μm. Particles ranging from 0.1 μm to 200 μm are found but it is estimated that 90 % of the particles are smaller than 100 μm. Bigger particles exist, though they are usually aggregates of fine particles (5-10 μm) covering larger ones [Machado *et al.* 2006, Makkonen *et al.* 2010, Rao 2006, Xia *et al.* 2000]. According to Kemperman [Kemperman 2010], the tendency of the dust to agglomerate is caused by exposure to air moisture.

Makkonen *et al.* [Makkonen *et al.* 2010] have analyzed the dust that were also studied in this thesis and reported that minerals like Cr_2O_3 were many times encapsulated inside a glass phase. They also detected other zonal particles where interesting components were enriched in the inner zones of the particle. Particles in the fine fraction instead did not show signs of encapsulation. From a hydrometallurgical point of view this phenomenon is very interesting. It is possible that the surrounding material hinders the leaching of desired minerals.

2.5 Problems and opportunities related to flue dusts

Stainless steel is a material whose demand is strongly connected to the rising standard of living around the world. Its demand is high in industrialized countries and growing rapidly in rising economies, like those of China and India (Figure 4). Since the 1950`s, the stainless market has been growing, on average at annual rate of 6 %. Some decline in the market was observed due to recent economic circumstances, but an output of 30 million tones was still estimated for the year 2010. With this level of output, the amount of generated dust would have been 750 000 tons [Meurer *et al.* 2001].

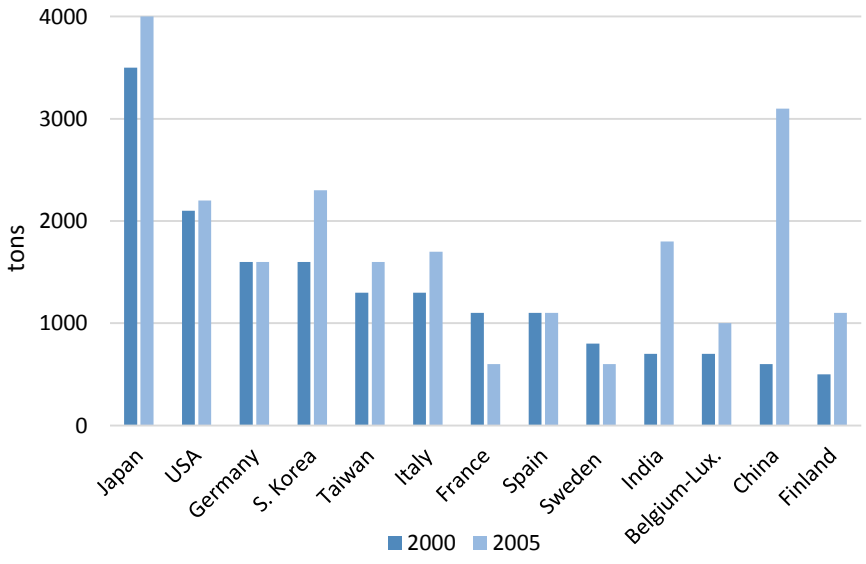

Figure 4. Stainless steel production, tons [Reck *et al.* 2010].

A few different processes are applied for producing carbon steel and stainless steel, but in the recent decades the Electric Arc Furnace process that has increased its share. The EAF process that uses a large proportion of recycled steel scrap as raw material, is nowadays regarded as the norm especially in stainless steel production. The proportion of scrap in stainless steel can technically be as high as 100 % of the charge, the global average being 60 %. Because of its efficiency regarding costs and energy consumption and as more and more steel scrap has become available to the market every year, the EAF process will likely continue to increase its popularity [Fujii 2005, Nakamura *et al.* 2008, Reuter *et al.* 2005, Schumacher *et al.* 2007, Zunkel 2001].

Some problems have arisen with growing production and scrap utilization rate. Recycled steel scrap contains other metals in addition to the main component that is iron. These metals can include zinc, chromium, nickel, molybdenum and lead; some of which are regarded as hazardous to human health and the environment. During steel production, they have a tendency to accumulate in the flue dusts that are generated in different parts of the process chain. 30-70 kg of dust is generated per ton of stainless steel produced, and it is estimated that stainless steel and carbon steel production generates a yearly amount of 1.7-2.0 Mt of EAFD in the US, Europe and Japan [Denton 2005, Zunkel 2001].

The high content of non-ferrous metals in the dusts becomes a problem as they make the dust unsuitable for direct recycling to the steel making process. Zinc is an element that causes most of the problems and its percentage should be reduced to 0.1 % so that dusts could be fed back to the EAF [Kemperman 2010, Ruetten 2010]. Halides in the dusts are detrimental to zinc electrolysis and make direct supply to zinc industry impossible [Maccagni *et al.* 2010]. The dusts can additionally contain chromium, lead, cadmium or arsenic and are therefore classified as hazardous waste. Hazardous waste has to be situated to a special landfill site or treated chemically to a less harmful form to prevent possible leaching of heavy metals to the environment. Dust´s hazardousness is normally evaluated based on the content of dangerous elements leached from it. In the EU, limit for Cr is 5 mg/l in a single sample [Environmental permit for Tornio Works], and in the US limits for Cr and Pb are both 5 mg/l [Laforest *et al.* 2006]. Stainless steel dusts usually exceed these limits and are also mentioned by the ministry of environmental affairs in Finland in a list of hazardous solid waste [Article 1129/2001]. The Finnish

legislation states that material that is to be landfilled to sites of relatively harmless waste cannot exceed the limits in Table 3.

Table 3. Limit values that are applied at finnish landfill sites [Article 331/31].

Element	Permanent site	Normal site
	Limit with L/S 10, mg/kg	Limit with L/S 10, mg/kg
As	0.5	2
Ba	20	100
Cd	0.04	1
Cr $_{tot}$	0,5	10
Cu	2	50
Hg	0.01	0.2
Mo	0.5	10
Ni	0.4	10
Pb	0.5	10
Sb	0.06	0.7
Se	0.1	0.5
Zn	4	50
Chlorides	800	15 000
Fluorides	10	150
Sulphates	1 000	20 000
Total Dissolved Solids	4 000	60 000

Viewing stainless steel flue dusts merely as waste is not a good approach. Steel companies around the world have recognized new reuse possibilities and the dusts potential as raw material. At the moment, some 6 % of zinc industry´s raw material is comings from flue dusts. When it is also noted that stainless steel dusts can contain valuable metals like nickel and molybdenum, and that landfilling is becoming more costly and regulated, the recycling becomes economically worthwhile. The competitiveness of a recycling process depends on the prices of alternative treatment methods and landfilling costs as well as the prices of recycled compounds. When landfilling is cheap there is no economic incentive for dust treatment. Recent tightening in waste legislation has created more pressure to investigate treatment methods for the future. Also, the fluctuations in alloying element prices and increasing demand of zinc by the galvanizing industry have made recycling more interesting. Molybdenum and nickel prices in January 2013, for example, fluctuated between 25 300-26 500 $/ton and

17 145-18 375 $/ton, respectively. The three month average price for zinc in the London Metals Exchange in January 2013 was 2 058.09 $/ton [London Metals Exchange]. It is estimated that concentrated zinc oxide could be sold for 70 % of the LME price of zinc, and other recycled metal alloys for 50 % of their LME prices [Antrekowitsch *et al.* 2010]. The current prices will obviously have a large impact on the profitability of dust recycling.

3 DUST TREATMENT PROCESSES

Some of the most important treatment processes that are used for removing zinc from the flue dusts are described and compared with each other in this chapter. Pyrometallurgical processes are introduced only superficially, while hydrometallurgical processes are described in more depth. In the end of the chapter, requirements for a viable treatment process are discussed.

3.1 Introduction to dust recycling processes

Steel making flue dusts can be treated either pyrometallurgicaly, hydrometallurgicaly or by using a hybrid process that consists of both pyrometallurgical and hydrometallurgical process steps. An ideal treatment process would separate valuable elements from the part that has no re-use potential, and would create only small amounts of waste material in a non-hazardous form.

A few of the treatment processes that have been tested or operate either commercially or on pilot plant scale are presented in Figure 5. Some of them produce high grade metallic zinc as the end-product while others produce an intermediate compound that can be used as raw material in zinc production. The majority of all commercialized treatment processes are pyrometallurgical, and the Waelz kiln for example is used worldwide in treating approximately 80 % of all EAF dusts [Ruetten 2010]. From hydrometallurgical processes, only the EZINEX process has reached commercialization but research on the field continues and new processes are in development [Nakamura *et al.* 2008, Zunkel 2001].

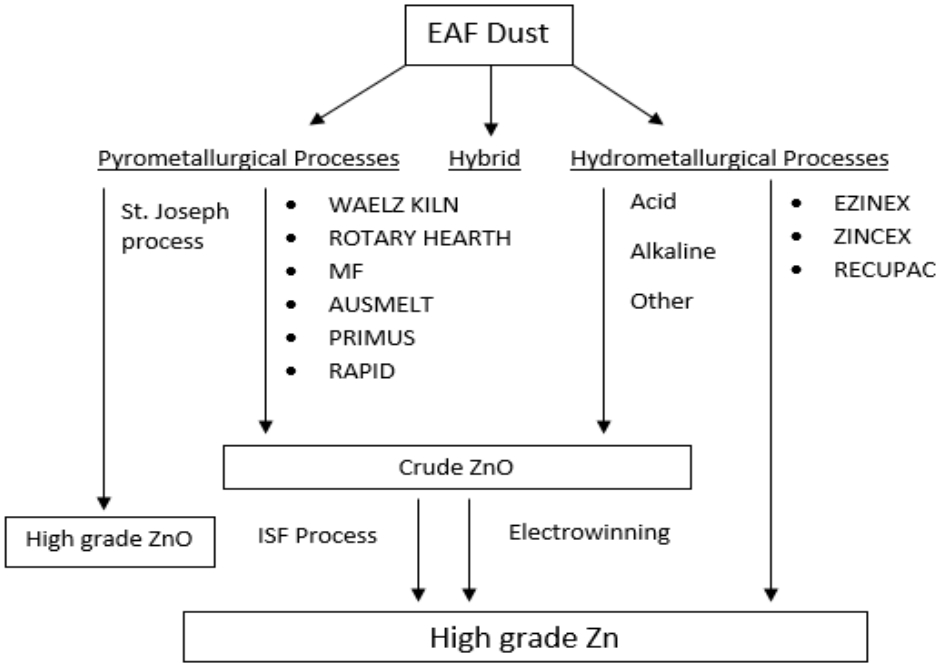

Figure 5. Comercialized and pilot plant treatment processes [Nakamura *et al.* 2008].

3.2 Pyrometallurgical processes

In pyrometallurgical processes, flue dusts are treated in a reducing atmosphere at high temperature, where zinc ferrites and zinc oxides are reduced, vaporized and oxidized back when the temperature in the off-gas system drops. A part from non-ferrous heavy metals, halogens (Cl, F) and alkalis (Na, K) are volatilized and also end up in the dust. Generally, it can be said that with pyrometallurgical processes, it is possible to recover zinc and lead as oxides and produce an environmentally neutral slag. On the other hand, these processes are energy intensive and require an off-gas cleaning system. Pyrometallurgical processes also need large amounts, minimum being close to 50 000 ton of high zinc-containing (2-18 %) raw material as feed in order to operate efficiently [Nyirenda 1991]. Economically speaking they are large investments and bind lots of operating capital. Pyrometallurgical processes for stainless steel dust treatment are well established and working. Until now the high energy consumption and operating costs have been canceled by the high value of end products [Meurer *et al.* 2001].

Waelz kiln, or the rotary kiln, is traditional and the most used process for treating flue dusts. Worldwide, around 80 % of EAFD is treated with the Waelz process and it is considered Best Available Technique (BAT) for treating carbon steel flue dusts [Meurer *et al.* 2001, Industrial Emissions Directive 2010/75/EU]. Other pyrometallurgical processes that are used on industrial scale include plasma reactor and flame reactor processes. One of the most modern plasma based processes is the PLASMADUST process that is, in fact, used in treating part of the dusts from Outokumpu´s Tornio Works, where the dust that were studied in this thesis originate from. The plasma process utilizes plasma gas to supply heat for reduction reactions and coke for reducing agent. The process takes place in a water-cooled shaft furnace at 4000-5000 °C. High temperatures enable reduction of iron, nickel, molybdenum and chromium with good yields (Fe, Ni, Mo 90-98% and Cr 80-95 %). The PLASMADUST process produces 100-200 kg of dust per 1000 kg of treated dust [Herlizt 1981, Meurer *et al.* 2001].

3.3 Hydrometallurgical processes

In hydrometallurgical processes, flue dusts are leached in a liquid medium. Processes aim at dissolving wanted metals from the dusts to the leachate, while undesired elements should remain in the residue. The pregnant leachate is purified from unwanted elements using precipitation, ion exchange or solvent extraction methods. Subsequently, the desired metal can be produced in a metallic form or as a salt by electrolysis or crystallization from the purified solution. The residue, which in the case of stainless steel dusts consists mainly of iron, is finally recycled back to the steel making process, landfilled or sold as by-product.

Zinc percentage in EAF steel making dusts can vary a lot; values from 2-40 % are found in literature [Meurer *et al.* 2001, Nyirenda 1991]. In stainless steel dusts, the percentage is less than in carbon steel dusts, only around 2-6 % [Nyirenda 1991], which is quite low regarding treatment by the pyrometallurgical route. Hydrometallurgy offers efficient processing alternatives for low-zinc dusts and can additionally treat smaller amounts of dust making it a suitable option for on-site dust treatment, especially in stainless steel production. Small scale on-site treatment of low-zinc containing dusts is thought to be the most economic and environmentally sound option, as treatment and transport costs are minimized [Nakamura *et al.* 2008]. The investment in the process

and the costs of running it are less than in pyrometallurgical treatment processes. A hydrometallurgical process is also more selective, meaning that different elements can be separated from the dust in different parts of the process. Hydrometallurgical processes can be divided into acid and alkaline, H_2SO_4 being the most commonly used acid, and NaOH (caustic soda) the most common alkali. Other usable leaching agents include HCl, HNO_3, $(NH_4)_2CO_3$ and acetic acid [Jha *et al.* 2001].

3.3.1 Acid leaching

Zinc oxides can be completely leached from stainless steel flue dusts by acid leaching at room temperature and atmospheric pressure. Moreover, hot acids are able to dissolve zinc oxide as well as refractory zinc ferrite [Arslan *et al.* 2003, Caravaca *et al.* 1994]. Leaching is not selective and because zinc ferrites are also dissolved, a later process step for iron removal is needed. The leachate can be purified from iron and other impurities such as Cd or Pb by different solution purification methods. Zinc metal can be produced from the purified leachate by electrowinning, or alternatively, zinc salt can be produced by crystallization [Jha *et al.* 2001].

Various acid leaching processes have been tested in pilot plants. The Modified Zincex process for instance consisted of leaching in dilute sulfuric acid followed by solvent extraction to produce an electrolyte for zinc electrolysis [Jha *et al.* 2001, Rao 2006]. The Cashman process used sulfuric acid and elevated pressure to leach zinc from arsenic containing raw material [Rao 2006, Xia *et al.* 2000].

Sulfuric acid is one of the most common acids that have been investigated in dust recycling. It is preferred because of its familiarity as well as low cost and availability. Other favorable properties of sulfuric acid include very low volatility and high chemical stability in aqueous solutions [Sohn 2006].

3.3.2 Alkaline leaching

Alkaline solutions can dissolve zinc selectively to iron, which means that only zinc oxide is leached and zinc ferrite will remain insoluble. This way, part of the zinc is lost in the process but an additional iron removal step can be avoided. The process can be advantageous in some cases, but it depends on the dust mineralogy. The amount of zinc that can be recovered with alkaline leaching depends on how much of zinc is bound to zinc oxides. The process yield can be remarkably enhanced if the dust is pre-treated pyrometallurgically so that zinc ferrites are reduced to zinc oxides. This way almost 100 % of total zinc can be recovered.

The only hydrometallurgical treatment process that is really operating in a commercial scale is the EZINEXprocess, which is based on alkaline leaching. In the process, ammonium chloride is used to solubilize zinc oxides at 70-80 ˚C temperature. The solution is then purified from cadmium and lead using cementation, and after that zinc can be extracted from the solution with electrolysis. [Jha *et al.* 2001].

Other common alkaline solution used in dust treatment is sodium hydroxide or caustic soda. It can selectively leach zinc oxides and leave iron to the residue. Caustic leaching has been tested on semi-pilot plant scale in the 1980´s. The Cebedeau process used concentrated (6-12 M) NaOH at 95 ˚C for 1-2 hours leaching. The process produced fine powder with 20 % zinc content but was eventually abandoned because of problems in the filtration stage [Jha *et al.* 2001]. Caustic leaching has been studied in METDUST project by Stefanova *et al*. [Stefanova *et al.* 2012 & 2013].

3.4 Requirements for a treatment process

Steelmaking flue dusts exist in various forms and the ideal treatment process depends mainly on the mineralogy of the dusts and each case has to be evaluated independently. Important factors to consider include the dust´s zinc content, the ratio of zinc oxide to zinc ferrite as well as content of valuable and hazardous elements.

There are some basic requirements for any hydrometallurgical treatment process that are widely known and referred to in literature and research papers [Heikkinen 2012, Kemperman 2010, Stefanova *et al.* 2012]:

- Desired metallic compounds have to be soluble in the leachate
- Metal recovery from leachate has to be economic
- Impurities have to be separable
- Leachate has to be easily regenerated and recycled
- Leachate cannot cause corrosion in the reactor
- Hazardousness of materials and products have to be minimized

4 THEORETICAL ASPECTS

This chapter deals with theoretical aspects that are relevant in different steps of the process. Important hydrometallurgical principles and their application in the experimental part of this thesis are outlined here.

4.1 Water washing

Water washing is designed to leach out chlorides that are predominantly present as water-soluble halides, potassium chloride (KCl) and sodium chloride (NaCl). Presence of species like lead chloride and zinc chloride that are insoluble in water is also possible.

The effect of leaching parameters has been investigated previously in several research papers [Bruckard *et al.* 2005, Caravaca *et al.* 1994, Chen *et al.* 2011, Kemperman 2010, Xia *et al.* 2000]. Bruckard *et al.* for example report removal efficiencies of 90-99 % for Cl and K, 50 % for Na and 10 % for Ca at ambient temperature. The study also indicates that halide leaching is complete between 30-60 min from the beginning of washing. Reported extraction efficiencies and the progression of leaching can be seen in Figure 6. They used L/S 3, but the L/S ratio has not been found to have a major effect on washing efficiency [Caravaca *et al.* 1994, Chen *et al.* 2011, Xia *et al.* 2000].

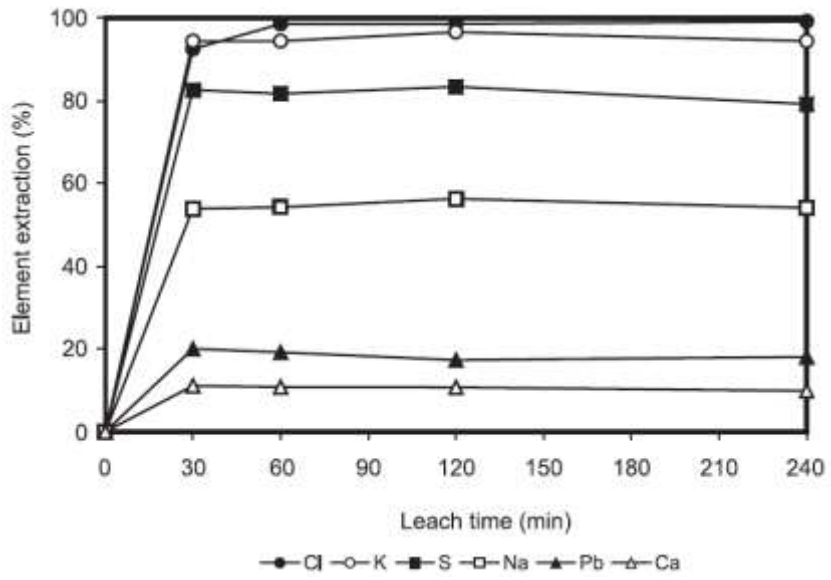

Figure 6. Extraction of elements in water washing at pH 12 and 25 °C reported by Buckard *et al.* [Bruckard *et al.* 2005].

4.2 Sulfuric acid leaching

Dissolution of zinc oxide and zinc ferrite in sulfuric acid takes place according to reactions (1) and (2):

$$ZnO\ (s) + H_2SO_4\ (aq) \rightarrow ZnSO_4\ (aq) + H_2O\ (l) \quad (1)$$

$$ZnFe_2O_4\ (s) + 4H_2SO_4\ (aq) \rightarrow ZnSO_4 + Fe_2(SO_4)_3\ (aq) + 4H_2O\ (l) \quad (2)$$

The dissolution of zinc and iron is dependent on the leaching conditions (i.e. potential and pH). Equilibrium areas for different zinc and iron species can be seen in E-pH – diagrams of the Fe-S-Zn-H_2O system at 25 °C and 100 °C (Figure 7 and Figure 8).

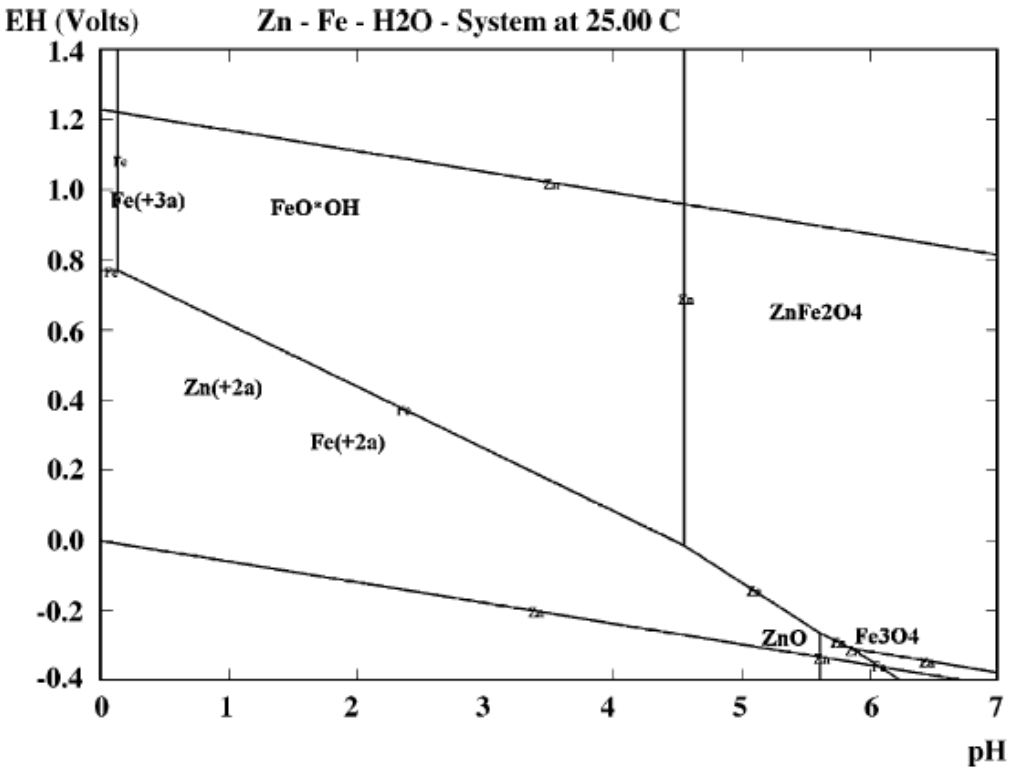

Figure 7. E-pH – diagram of Fe-S-Zn-H2O system at 25 °C [Havlik *et al.* 2006].

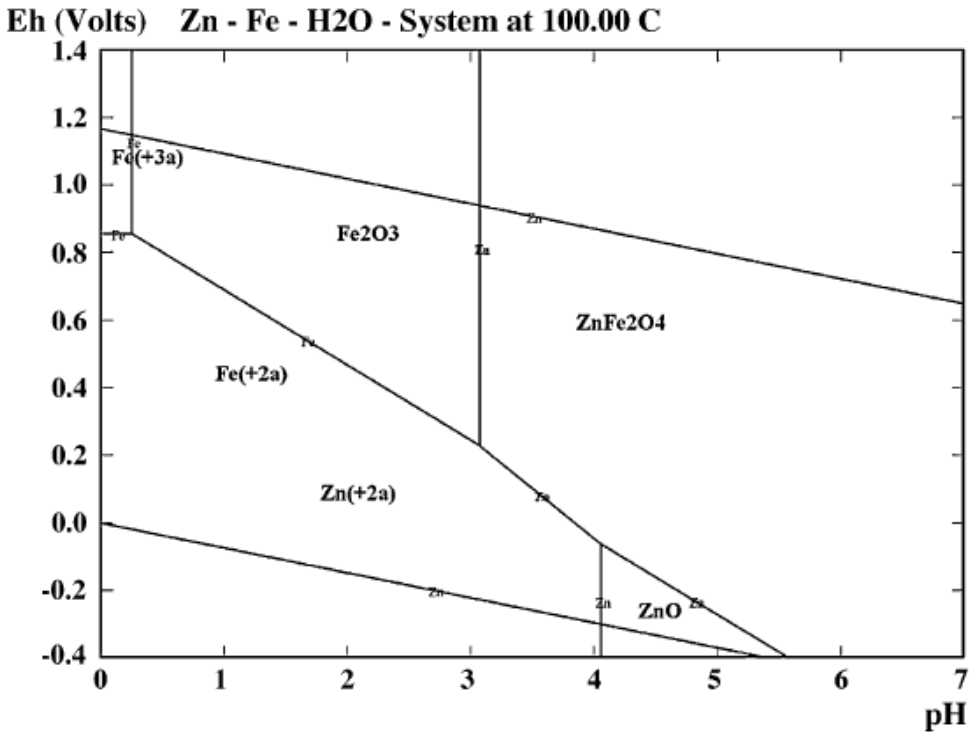

Figure 8. E-pH –diagram of Fe-S-Zn-H2O system at 100 °C [Havlik *et al.* 2006].

Experiments dealing with sulfuric acid leaching usually reached high zinc removal rates. Most of the experiments were done using 0.1-1.5 M sulfuric acid and the highest tested acid concentration was 3.5 M [Reyad 2010]. Dilute acid can only leach zinc oxides, so yield were lower than when more concentrated acid was used. With concentrated acids, zinc ferrites are also leached but selective leaching of zinc is hindered.

According to Langova *et al.* [Langova *et al.* 2007], almost 100 % zinc extraction can be achieved with 3 M sulfuric acid leaching after 6 hours with liquid/solid ratio 5 at 80 °C. In those conditions, some 90 % of iron was also leached. When a diluted (0.1-0.3 M) acid was used, less zinc was extracted than with concentrated acid, but more selectively to iron: some 30 % of zinc was leached while the zinc/iron ratio was reported to be 9.

Kekki *et al.* [Kekki *et al.* 2012] have previously studied the same kind of dusts that were used in this thesis. They tested the effect of leaching parameters (pH, acid concentration, temperature and L/S ratio) on maximum and selective leaching of zinc in a similar experiment set up. They report that maximum leaching (65-100 %) was

achieved with 1.5 M sulfuric acid, 90 ˚C and L/S ratio 10. Best selectivity regarding Fe, Cr, Ni and Mo was found with 0.5 M acid, 30 ˚C and L/S 10. 33-72 % of zinc was leached with the previous parameters.

Referring to previous studies [Caravaca *et al.* 1994, Cruelles *et al.* 1992, Havlik *et al.* 2006, Herrero *et al.* 2010, Kekki *et al.* 2012 & 2011, Kelebek *et al.* 2004. Langova *et al*. 2007, Majuste *et al.* 2008 & 2009, Oustadakis *et al.* 2010], it is widely observed that that by increasing temperature, acid concentration and L/S ratio, higher zinc extraction can be reached and leaching will be faster. Some of the reported results are presented in Table 4.

Due to the alkalinity of the flue dusts, the leaching reaction in acid is highly exothermic [Kelebek *et al.* 2004] and as the dust dissolves, the pH of the solution will rise. pH control is needed in order to keep the system in an area where zinc species are soluble. If the pH rises too high leached zinc will start to precipitate back and extraction will be lower. Iron precipitation on the other hand would be advantageous to the process.

Table 4. Reported zinc removal rates in selected research papers.

Reference	H_2SO_4 (mol/l)	pH	T (°C)	Time (min)	Zn extraction (%)	Additional information
Caravaca *et al.* 1994	5		25	120	70 -80	-
Cruelles *et al.* 1992	-	-	23	-	80	Low acid concentration, non- magnetic fraction of EAFD flue dust.
Havlik *et al.* 2006	0.5	-	70	60	60-100	L/S ratio 10-25.
Herrero *et al.* 2010	-	3.5	-	120	82.7	Two stage leaching, stage 1.
Herrero *et al.* 2010	-	3.5	-	60	80.1	Two stage leaching, stage 2.
Hoang Trung *et al.* 2011	1.0	-	80	60	80	Blast oxygen furnace flue dust.
Kekki *et al.* 2012	0.1 -1.5	-	90	120	30 -100	Stainless steel flue dusts.
Kelebek *et al.* 2004	3	~ 2	-	-	81	Dust from the coarse fraction (i.e. > 39 µm).
Langova *et al.* 2007	0.1 – 3.0	-	80	360	30 -100	-
Reyad 2010	0.1	-	50	-	72	-

4.3 Subsequent processing for zinc recovery

Leachates from dust treatment contain impurities that have leached simultaneously with zinc. Before the leachates can be used in zinc production they have to be purified from possible traces of iron, lead, cadmium and nickel, for instance. Several different methods are used in removing these impurities from the leachates. The process of separating the impurities from the liquid phase by precipitation and filtration is one of the most challenging unit processes in hydrometallurgy.

Different impurities are typically removed separately in order to gain a product of higher purity and value [Herrero *et al.* 2010, Zunkel 2001]. Concentration limits for impurities in electrolytic feedstock are presented in Table 5.

Table 5. Concentration limits for impurities in electrolytic feedstock [Herrero *et al.* 2010].

Metallic impurity	Maximum concentration, ppm
Chlorine	0.05
Fluorine	0.10
Cadmium	0.20
Sodium	0.10
Iron	2.30
Aluminum	0.30

Iron is the most predominant impurity and can be removed from the solution by one of the four processes: goethite process, hematite process, jarosite process or magnetite process. The first three are used on industrial scale in electrolytic zinc production. [Arslan *et al.* 2003, Burkin 2001 p.130]. Regarding operation pH and temperature, the goethite process works in the mildest conditions. A schematic picture of the goethite process is shown in Figure 9. The process operates at atmospheric pressure, 80-90 °C temperature, pH range 2-4 and maximum iron concentration of 1 g/L. The pH is already in suitable are for treating acid solutions.

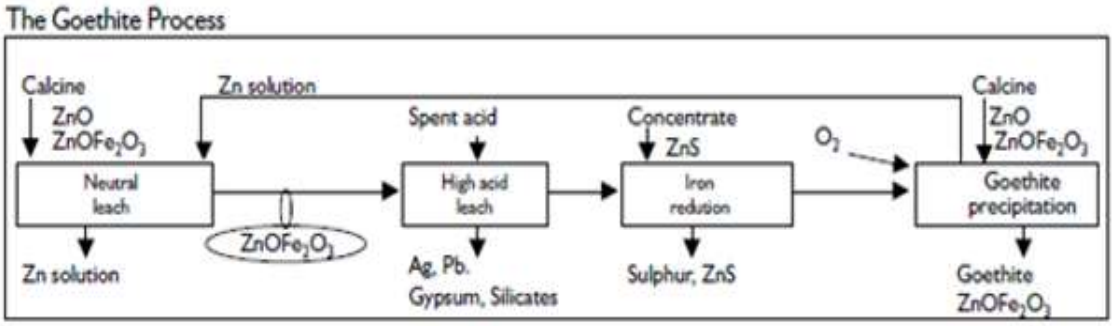

Figure 9. Goethite process flow sheet (Heikkinen 2012).

In the process, oxidizing agents are applied to oxidize Fe(II) into Fe(III) that precipitates at more favorable pH area (< pH 2.2) in acid leaching [Herrero *et al.* 2010, Langova *et al.* 2007, Aromaa 1990]. After oxidization, the pH of the solution is adjusted to an area where the hydrolysis reaction of Fe(III) can occur according to reaction (3).

$$Fe^{3+} + H_2O \rightarrow Fe(OH)^{2+} + H^+ \quad (3)$$

Iron percipitates as goethite (α-FeOOH), akagenite (β-FeOOH), lepidicrocite (γ-FeOOH) or hematite (Fe_2O_3) together with amorphous phases [Burkin 2001 p.130, Langova *et al.* 2007]. The iron compounds are can be recovered by recycling the precipitate back to steel making process. For this to be possible, the precipitate should contain less than 1 % zinc [Jha *et al.* 2001].

Iron removal in the Goethite process is based on the fact that metallic hydroxides precipitate in a very narrow pH area [Aromaa 1990]. Hydroxide precipitation can be applied also in removing other metallic species from the solution according to reaction (4):

$$Me^{n+} + n\ OH^- \rightarrow Me(OH)_n \quad (4)$$

As an alternative to hydroxide precipitation, the desired metals can be removed as sulfides according to reaction (5). Sulfide precipitation is used, for instance, in the production of nickel and cobalt [Aromaa 1990].

$$Me^{2+} + H_2S \rightarrow MeS + 2H^+ \quad (5)$$

Other undesired species such, as Pb or Cd, can be removed by cementation that takes place according to reaction (6):

$$Zn + Me^{2+} \rightarrow Zn^{2+} + Me \quad (6)$$

The same method can also be used to remove valuable alloying elements Ni and Mo. In practice, cementation is done by adding zinc powder to the solution where it causes the

reduction of desired metallic ions. To reduce the ion to metallic state the potential has to be set below the line of thermodynamic equilibrium between the metal and its ion. Stability areas of different metallic ions can be determined from E-pH diagrams. Elements can additionally be removed from solution by adjusting temperature so that their solubility is minimized. The excess will then crystallize and can be removed by filtering. Same can be achieved if the solution is evaporated. After purification steps, the leachates can be used in zinc production that is often done using electrolysis. Nickel is another metal that can be recovered electrolytically from solution.

5 RAW MATERIAL DESCRIPTION

Characteristics of the flue dusts that were studied in this thesis are described in this chapter. Chemical and mineralogical composition and particle size distribution described in general and separately considering all five dust samples.

5.1 General observations

The five dust samples came from Outokumpu´s Tornio Works stainless steel plant in Northern Finland. The samples were taken from different parts of the process in 2009 and have been analyzed in Oulu University´s CIRU center as well as in Technical University of Oulu [Makkonen *et al.* 2010] and Technical University of Kosice in Slovakia [Havlik *et al.* 2010] to attain knowledge of their chemical composition, mineralogy and general characteristics. Additional chemical analyses were done in a private laboratory in Espoo [Labtium Oy]. Generally, all samples had a very complex chemical and mineralogical composition. This heterogeneity together with the sample´s small particle size made definite analysis challenging in many cases and should be kept in mind while interpreting the results. The samples were marked with following abbreviations that are be used in this thesis (Table 6):

Table 6. Sample ID and origin.

Sample ID	Origin of sample
CRK1	Chrome converter
VKU1	Electric arc furnace, line 1
VKU2	Electric arc furnace, line 2
AOD1	Argon oxygen decarburization converter, line 1
AOD2	Argon oxygen decarburization converter, line 2

Mineralogical analysis was done in Oulu using XRD (x-ray diffractiometer), light microscope and SEM (scanning electron microscope) and EPMA (electron probe micro analyzer). With XRD it could be detected that chromite was an important phase in all samples. Other phases were difficult to identify with 100 % certainty because of overlapping spikes and data lacking from XRD library. The XRD is also incapable of

identifying phases that have a concentration less than 1 % or amorphic phases such as glass. Typical mineralogical phases that have been identified in different studies were presented in Table 2.

Grain size distribution was measured using a series of sieves as well as Coulter-analysis (Beckman Coulter LS 13 320 type). Sieving only worked for CRK while the sieves were blocked by other samples. The blocking was explained by fine particles congesting the holes in the sieve. Grain size distribution curves show that particles over 30 µm wouldn't exist in large amounts even though their presence was observed with a microscope. This difference might be explained by the small samples that were used in Coulter analysis. Bigger particles might not have been present in the sample or they might have sunk rapidly and therefore not detected by the analyzer. Detailed analyses of the samples particle size distribution are found in Appendices 1-10.

The microstructure of all samples consisted of bigger particles that were surrounded by finer material. Bigger particles were found out to be very different in shape, ranging from spherical to angular and to porous. They consisted often from grains of one or more phases that were enclosed in a glass phase. The finer particles were mainly 5-10 µm but the smallest grains had a diameter well below 1 µm. The smallest particles were almost invisible in SEM and their microstructure is left partly unclear [Makkonen *et al.* 2010]. Microscopic views of the fine fraction are shown in Figure 10.

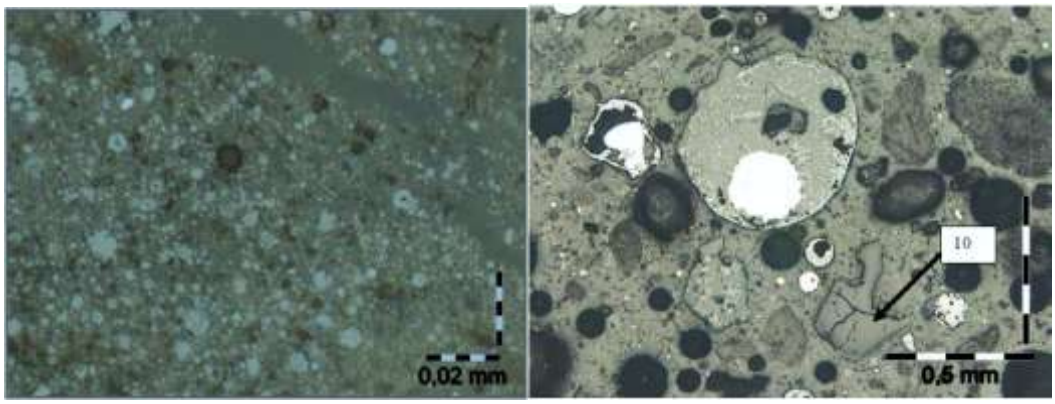

Figure 10. Microscopic views of the fine fraction [Makkonen *et al.* 2010].

All dust samples contained iron as principal element, mostly as different oxides. Depending on the process as well as raw material and additives, other elements were present in variable amounts. Zinc, which is of particular interest, originated from scrap and is present mainly as zinc oxide and zinc ferrite ($ZnFe_2O_4$). Calcium, potassium, magnesium and halides come from slag and fluxes, whereas nickel, chromium, molybdenum and manganese are used as alloying elements in stainless steel production. Additionally, small amounts of other elements were found but their percentage was negligibly small. Chemical compositions of dust samples are presented in Table 7. Analysis were done by Labtium Oy using ICP-OES method.

Table 7. Samples chemical compositions and estimated standard deviations.

	CRK		**VKU1**		**VKU2**		**AOD1**		**AOD2**	
	mg/kg	SD %	mg/kg	SD %	mg/kg	SD %	mg/kg	SD %	mg/kg	SD %
Ca	175000	9	106340	4	136000	4	48270	6	152340	5
Cl	388	-	734	-	10600	-	644	-	531	-
Cr	140000	-	96000	-	102000	-	97400	-	97900	-
Fe	156000	43	194670	17	170670	16	351000	9	233340	12
K	2250	68	12770	5	13740	2	8320	10	8140	6
Mg	68200	6	24070	11	11350	22	12240	4	24370	3
Mn	2570	52	28170	16	23500	27	22600	20	25100	31
Mo	160	89	240	3	1350	5	280	14	13500	4
Ni	820	27	12200	25	21140	21	5900	19	27340	12
Zn	72100	5	73370	9	47840	21	99670	7	44370	8

Zinc, nickel, molybdenum and chromium were of special interest in this thesis. It can be seen from the table above and was also observed by Makkonen [Makkonen *et al.* 2010] that:

i. CRK has the highest content of chromium oxide

ii. Highest contents of NiO were found from VKU2 and AOD2

iii. Highest zinc contents were found from CRK, VKU1 and AOD1

iv. AOD2 had the highest MoO content

5.2 CRK dust

Spherical particles consisting of two different phases were identified as well as phases that contained Fe-Cr and Mg-Cr enclosed inside a glass phase. Fe-Cr particles that were not enclosed were also found and Si was present in these structures.

Detected angular particles consisted of Fe-Si and Si phases. Some of the low-chromium structures next to chromite had NiO content between 2-10 %. Particles with iron oxides and low in Cr_2O_3, ZnO, NiO and MoO_3 were observed. Some particles that resembled slag contained spinel and magnesio-chromite-spinel-series and had a higher Cr content (32 %). Some spherical particles with elevated Cr % were detected as well as particles that maybe consisted of calcite and fluorite.

The fine fraction of particles contained Cr_2O_3 and ZnO surrounded by other phases that could be rich in MgO, SiO_2 or CaO. Grains that were rich in Cr or Zn were almost always surrounded by pores and there was no capsuling phenomenon like in the case of larger particles. The fine fraction had the highest ZnO concentration. [Makkonen *et al.* 2010]

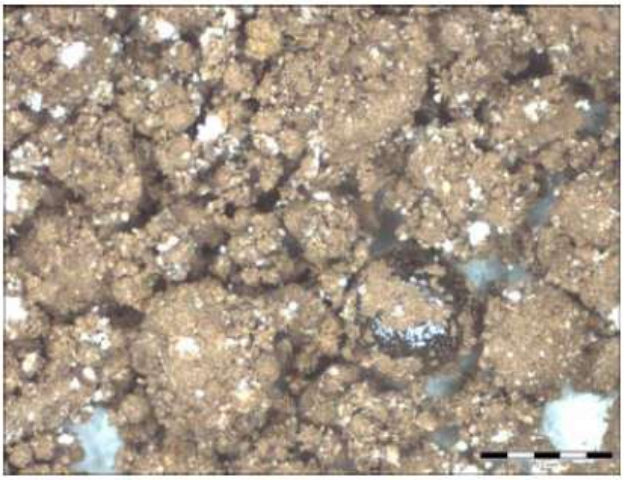

Figure 11. 63 x magnification of dust sample [Havlik *et al.* 2010].

5.3 VKU1 dust

The dust sample contained yellow angular and spherical particles of heterogenic consistency. The phases consisted of mainly iron and chromium together with small amounts of silicon. In this sample all chromite-like phases were labeled as magnesio chromite, unlike in the case of CRK which contained also actual chromite. The magnesio chromite in this dust is present enclosed in a glass phase. The chromite phase has over 40 % Cr_2O_3 content and ZnO content of 5-8 %. In the surrounding glass phase the ZnO percentage is around 4%. Cr-Fe-oxide crystals with varying amounts of NiO (0-4 %) and ZnO (0.3-8 %) were found to be present. Particles that probably originated from slag contain metal droplets, silicates and spinel group oxides. The spinel grains are rather rich in Cr_2O_3 (~20 %). MgO was also indentified.

The fine fraction of VKU1 had such a small particle size that SEM resolution was not sufficient so the analysis has been affected by surrounding coarser particles. What could be observed from the fine fraction was that it contained small amounts of SiO_2, CaO, MgO, MnO and Na_2O. Some grains in the fine fraction had relatively high percentages of Cr_2O_3 (2-38 %) and ZnO (2-23%). NiO was found present mostly below 1 %. [Makkonen *et al.* 2010]

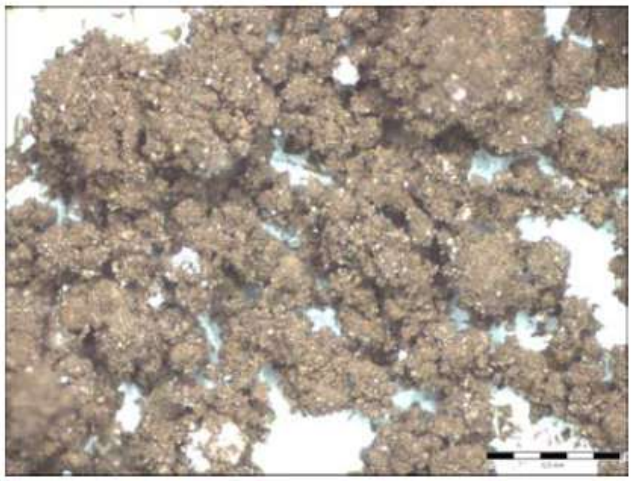

Figure 12. 63 x magnification of dust sample [Havlik *et al.* 2010].

5.4 VKU2 dust

Yellow angular and spherical particles similar to those in VKU1 were detected. Magnesio chromite was found to be enclosed in a glass phase and had higher Cr_2O_3 content (50-60 %) than the surrounding glass. NiO and ZnO were detected, highest 2 % in some grains. Some 15 % Al_2O_3 was also present in the glass. Some particles that had a zinc oxide percentage as high as almost 70 % were found.

Particles that originated from slag contained metallic droplets, silicates, oxide spinel and magnesio chromite inside them. Metal droplets consisted of Fe (61 %), Cr (10 %) and Ni (2 %). Cr_2O_3 content in the spinel was 19 % and 67 % in the magnesio chromite.

Fine fraction was again too small for an accurate SEM analysis. Still it could be observed that same kind of capsuling phenomenon as for larger particles didn't exist. This was also observed with CRK fine fraction. According to SEM, the fine fraction consisted mainly of FeO, Cr_2O_3, CaO, SiO_2 and ZnO. ZnO content in some samples was observed to be as high as 18 %. [Makkonen *et al.* 2010]

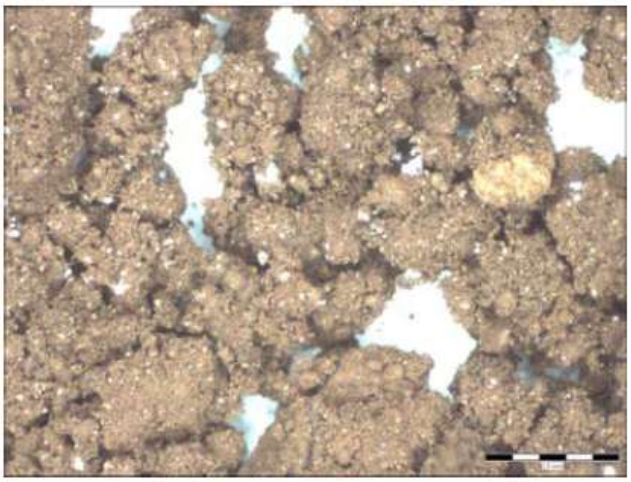

Figure 13. 63 x magnification of dust sample [Havlik *et al.* 2010].

5.5 AOD1 dust

The sample contained angular particles that consisted of two phases. One of the phases was yellow and the other bluish. The yellow phase contained iron and silicon that refers to ferrosilicon, whereas the blue phase contained mainly silicon. Spherical yellow particles that were sometimes agglomerated and sometimes homogenous were detected. They consisted mostly of Fe and Cr, but had around 2-3 % Ni. Chromite and magnesio chromite were found enclosed in a glass phase. Magnesio chromite was high in Cr_2O_3 (72-74 %). The surrounding glass phase contained 2-10 % Cr_2O_3. Cr_2O_3 phases had varying Cr_2O_3 and FeO content. NiO content was little bit over 1 % in the glass phase and zinc oxide content was lower than 6 %. Porous particles that had partly high ZnO percentage (some 16 %) were detected. They contained also Cr_2O_3, MgO, FeO and CaO. Slag particles with metallic droplets (Fe), silicate glass and oxide chomite and Cr-Fe oxide were found. Chromite phase had about 68 % Cr_2O_3 and zinc content was 5 % the highest. Some single grains whose composition is similar to periclase (MgO) and fosterite (MgO and SiO_2) were found as well as a round particle that was possibly fluorite (Ca and F).

Fine fraction was again too small for an accurate SEM analysis. According to microanalysis it contained MgO, CaO, SiO, Cr2O3, MnO, FeO and ZnO. In some cases the ZnO content was as high as 13.9 %, but mostly around 1 %. [Makkonen *et al.* 2010]

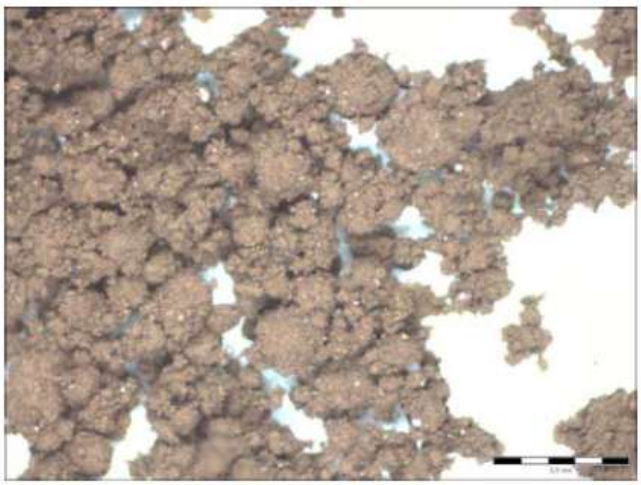

Figure 14. 63 x magnification of dust sample [Havlik *et al.* 2010].

5.6 AOD2 dust

The sample contained round and angular particles that often consisted of two different phases. Round particles were found out to be yellow and blue whereas angular particles were yellow-brown and blue. Both phases in the round particles contained iron and silicon, as did the yellow brown phase in the angular particles. The blue phase in the angular particles contained mainly (~93 %) silicon. Fine grains that surrounded bigger ones contained chromium, iron and silicon. Amounts of iron and chromium varied between 0.1-39 % and 16-67 %, respectively. Some of the particles contained also nickel (4-9 %). A mineral resembling chromite was found in shredded particles together with Cr-Fe oxide and glass. In addition to chromite, the dust contained magnesio chromite that was encapsulated in a glass phase as well as particles originating from slag that contained metal (Fe or Ni), glass and Cr oxide. As an exception to the other dusts, this dust contained phases that were rich in molybdenum (14-86 % MoO_3). Individual grains of probably wustite (FeO) and quartz or tridymite (SiO_2) were also observed.

Fine fraction was again too small for an accurate SEM analysis. Microanalysis revealed that MgO, SiO_2, CaO, Cr_2O_3, MnO, FeO, NiO and ZnO were present. ZnO content varied from 0.5 to 13.5 %. [Makkonen *et al.* 2010]

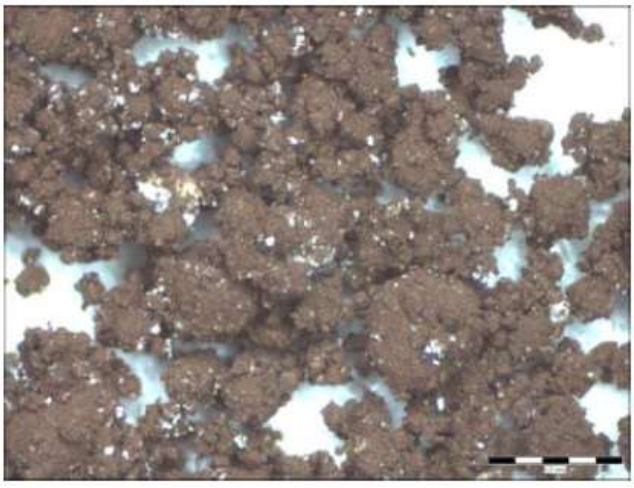

Figure 15. 63 x magnification of dust sample [Havlik *et al.* 2010].

6 EXPERIMENTAL METHODS

The process that was tested in thesis consisted of three steps. Each step was designed so that different elements could be leached out separately. The methods and the apparatus that were used are described in this chapter.

6.1 Water washing

Experiments were started with preliminary water washing tests so that ideal washing conditions could be established. The tests were carried out only for two samples, CRK and VKU1, and washing was studied at room temperature, at 50 °C and at 80 °C. Both samples were first dried for 24 h at 105 °C and then mixed with distilled water in a decanter glass that was placed on a heater disk. The decided liquid to solid ratio was 5; in this test 250 ml of water to 50 g dust. After mixing water with dust, stirring at 600 rpm was started using a magnetic stirrer. Temperature, pH and conductivity of the slurry were measured with VWR Phenomenal 111, first after 2 minutes and then every 10 minutes until the end of the test at 60 minutes. After 60 minutes of mixing, the slurry was filtered and the filter cake was dried at 105 °C for 24 hours. Samples were taken from each wash and the leachate and the dried filter cake were sent to analysis.

Based on preliminary tests and other research [Bruckard *et al.* 2005, Kemperman 2010], the actual water washing was decided to be done at room temperature (23 °C) and according to the previous procedure. The only difference was that larger amounts of dust were washed (i.e. 2500 ml / 500 g dust).

6.2 Leaching

Optimal leaching conditions (L/S-ratio, pH, temperature, agitation) and different sulfuric acid concentrations have been investigated in connection with the METDUST project and the conditions that were chosen to be tested in this thesis are based on that research [Kekki *et al.* 2011 & 2012].

6.2.1 First leaching step

Solid residue from water washing was treated further in this process step. 150 g of washed dust was leached with 750 ml 0.5 M sulfuric acid, keeping L/S 5 as previously. Leaching was carried out in a 1000 ml batch reactor (Figure 16), whose temperature was controlled using a heated water bath. Acid was first added and dust was introduced when the temperature in the reactor reached 90 °C. After adding the dust, mixing with a mechanical stirred at 300 rpm was started. The pH of the slurry was measured with a Lange sc100 Universal Controller and kept below pH 4.5 with a connected $NaOH/H_2SO_4$ -pumping system. Duration of the first leaching was 15 minutes, after which the slurry was poured out of the reactor and filtered with a double filter paper (type: Munktell, quality 00M) for 12 hours. The filter cake was then dried at 105 °C for 24 hours. Samples of the filter cake and the leachate were taken and sent to analysis.

6.2.2 Second leaching step

The second leaching was done with the same apparatus as the first leaching. 200 ml of acid was heated to 90 °C and mixed with 40 g of dust from the first leaching step. Two different acid concentrations, 2 M and 6 M, were used. Samples were taken with simultaneous measuring of pH (VWR Phenomenal 111) at 10, 60, 120 and 240 minutes. Before taking the samples (~20 ml), stirring (300 rpm) was turned off for 30 seconds so that the solid part of the slurry would sink to the bottom and a clearer liquid sample could obtained. Samples were then filtered using a double filter paper. The final sample at 240 minutes consisted of the whole remaining slurry and was suction-filtered. Samples were taken from the liquid part as well as from the dried filter cake (105 °C, 24 h).

Figure 16. Cell reactor with appliances. 1= mechanical stirrer, 2 = opening for $NaOH/H_2SO_4$ –pumping, 3 = thermometer, 4 = pH meter, 5 = condenser.

7 RESULTS

Results from the experiments are presented in this chapter. Zinc removal is discussed first followed by an overview in extraction of other elements during the process. Finally, the compositions of solid residues from different process steps are presented.

7.1 Zinc removal during the process

The main objective of the thesis was to remove as much of the zinc in the dusts as possible by a three stage leaching process. The first step was designed to remove only halides with a simple water washing procedure. Water washing was followed by two leaching steps. The first leaching was done using 0.5 M sulfuric acid and the second leaching was done using either 2 M or 6 M sulfuric acid. All samples went through both process options.

Zinc removal was assessed by monitoring Zn concentrations in the solid phase after each process step. Figures 18 and 19 depict the change in the dusts Zn concentration as the sample went through the process. Figure 17 shows results when the second leaching was carried out in 2 M acid and Figure 18 when it was done in 6 M acid respectively. As the recovery of zinc is done from the liquid phase, concentrations in leachates from each process step are presented in Table 8.

With 2 M sulfuric acid, zinc was leached: CRK 62 %, VKU1 58 %, VKU2 50 %, AOD1 61 % and AOD2 59 %. With 6 M acid the corresponding values were 58 %, 47 %, 43 %, 58 % and 44 %.

Table 8. Zinc concentrations (mg/l) in leachates from each process step.

	Water washing	First leaching	Second leaching_2 M	Second leaching_6 M
CRK	4.0	0.6	20660	14140
VKU1	4.3	3770	24900	13130
VKU2	2.7	1310	11070	9910
AOD1	5.2	11100	13330	17600
AOD2	7.5	1220	12250	11730

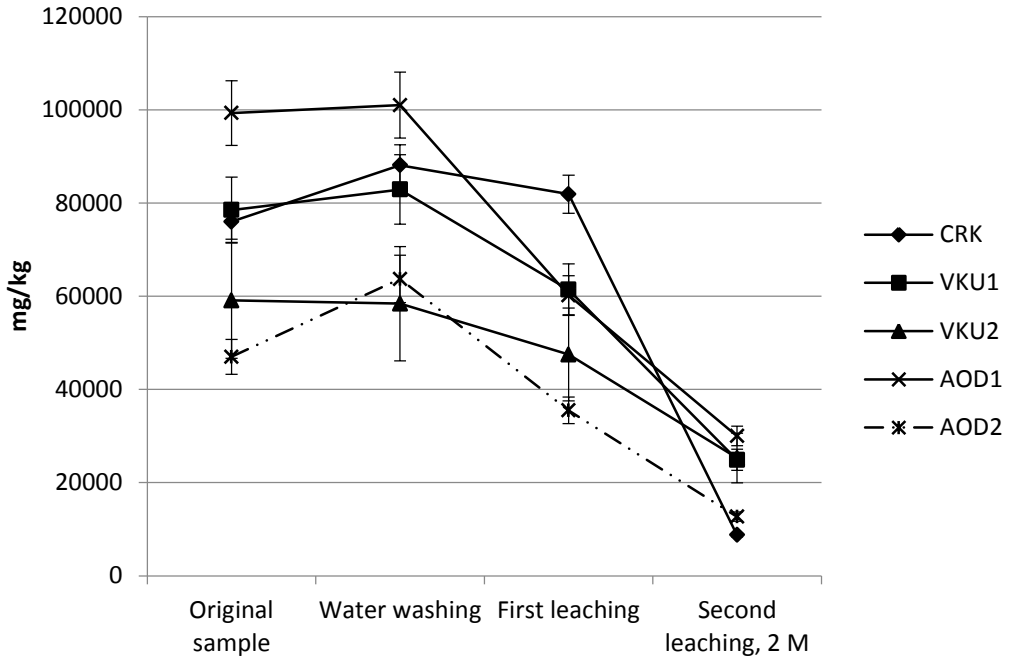

Figure 17. Zinc concentrations (mg/kg) in original samples and in solid residues after each process step. Second leaching was done using 2 M sulfuric acid.

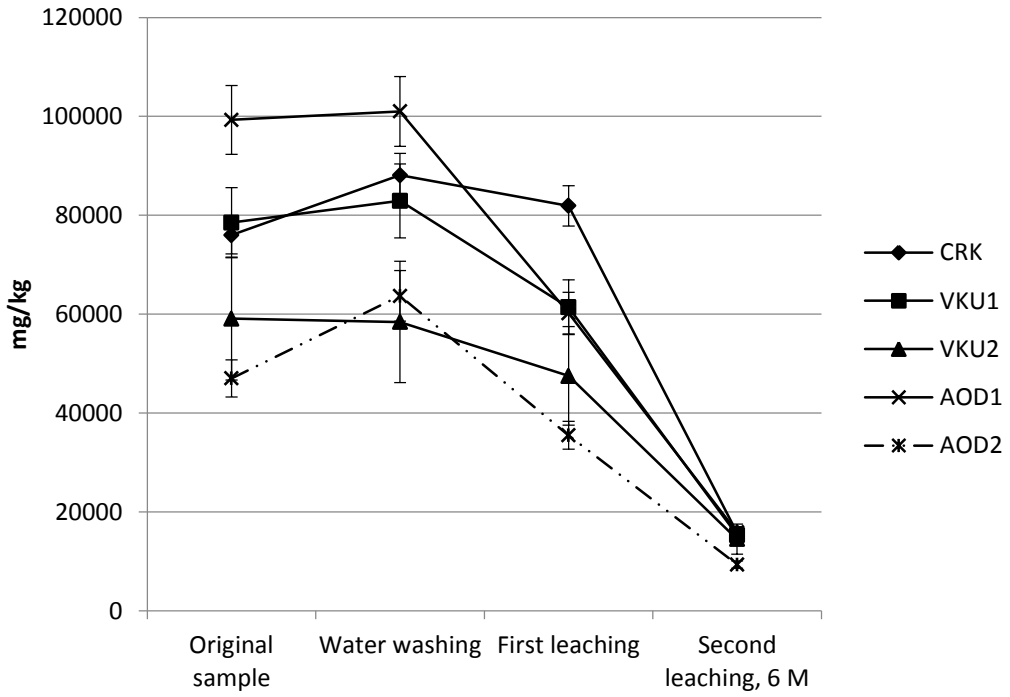

Figure 18. Zinc concentrations (mg/kg) in original samples and in solid residues after each process step. Second leaching was using in 6 M sulfuric acid.

7.2 Extraction of other elements during the process

7.2.1 Preliminary water washing tests

Preliminary water washing tests predicted that 60 minutes water washing could reduce chlorides by 80-90 % , potassium by 30-60 % and calcium by 3-10 % (Figures 19 and 20). During preliminary tests, a decrease in pH with time was observed for both samples at all temperatures (Figure 21). Solution conductivities instead showed no remarkable change (Figure 22). Halide extraction was not found to be dependent on the temperature so the actual water washing was decided to be done at ambient temperature (23 °C). Solid samples were analyzed using agua regia and ICP-OES technique. Liquid samples were also analyzed with ICP-OES.

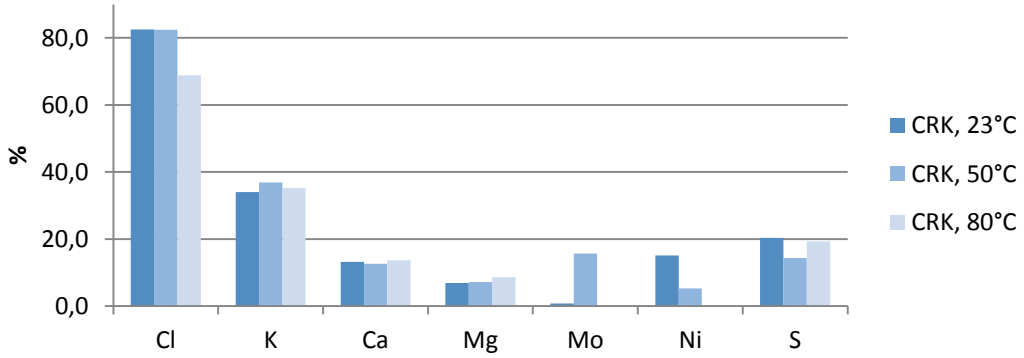

Figure 19. Extraction efficiencies (%) in preliminary water washing tests for CRK.

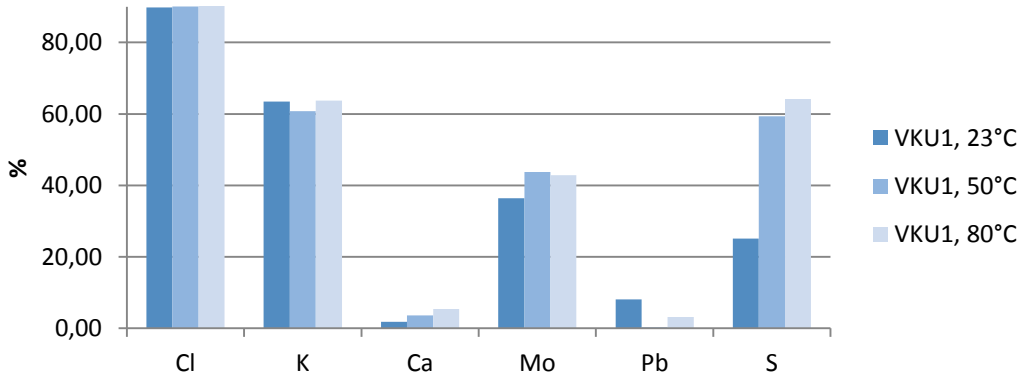

Figure 20 Extraction efficiencies (%) in preliminary water washing tests for VKU1.

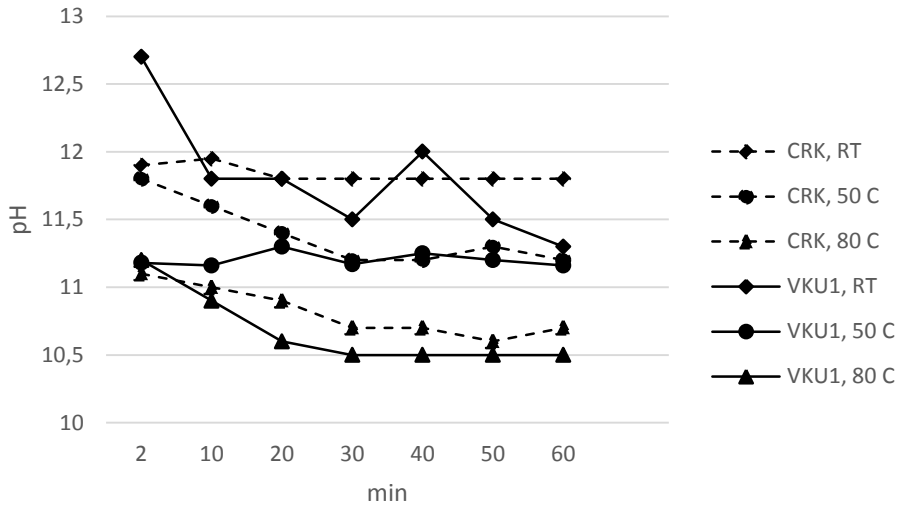

Figure 21. pH during preliminary 60 minute water washing tests at different temperatures for both samples (CRK and VKU1). RT = room temperature 23 °C.

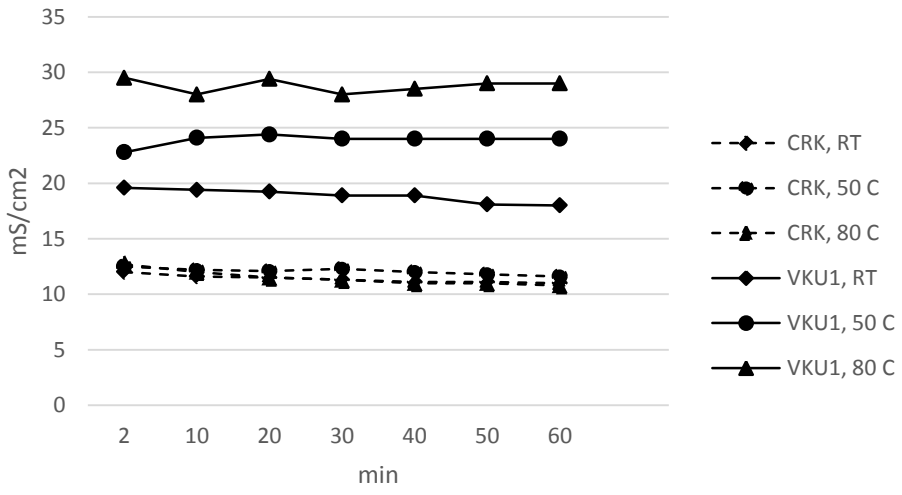

Figure 22. Conductivity during preliminary 60 minute water washing tests at different temperatures for both samples (CRK and VKU1). RT = room temperature 23 °C.

7.2.2 Water washing

Water washing was carried out in distilled water at ambient temperature (23 °C). 500 g of dust was mixed with 2500 ml distilled water (L/S 5) in a decanter and stirred at 600 rpm in a decanter glass for 60 minutes. After washing the slurry was filtered and dried. Extraction efficiencies for elements in this process step are depicted by Figure 23. Highest removal rates were observed for Cl, K, Ca and Mo. Percentages were determined by comparing the amounts of elements present in the leachate to the amounts in the solid sample before water washing. Concentrations of elements in leachates from this process step are presented in Table 9. Solid samples were analyzed using sodiumperoxide and ICP-OES technique. Liquid samples were also analyzed with ICP-OES.

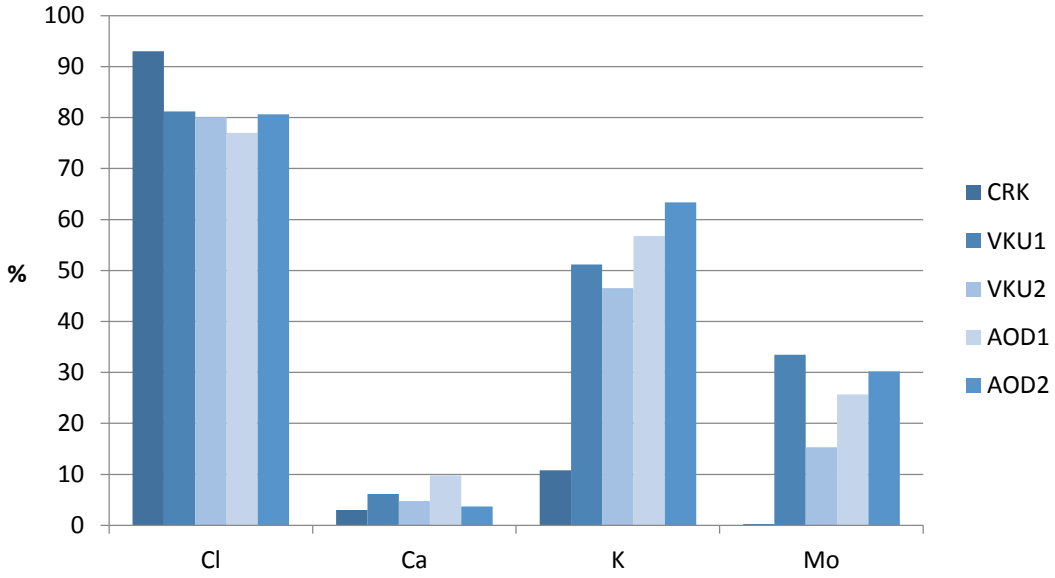

Figure 23. Extraction efficiencies (%) in water washing.

Table 9. Concentration of elements (mg/l) in leachates from water washing. Error estimate ±11 %.

	CRK	VKU1	VKU2	AOD1	AOD2
Cl	80	1490	2020	120	110
Ca	1090	1610	1490	1110	1350
Cd	-	-	-	-	0.01
Cr	16	150	200	210	150
Fe	0.10	0.14	-	0.23	-
K	100	1730	1550	1250	1350
Mo	0.17	20.0	52	20.0	1000
Ni	-	-	-	-	0.05
Pb	0.12	0.48	-	-	-
S	35	790	390	-	180
Zn	4.0	4.30	2.70	5.20	7.50
F	1.50	1490	3.80	7.70	5.10

7.2.3 First leaching

Leaching was carried out with 0.5 M sulfuric acid in a 1000 ml batch reactor at 90 ˚C, 15 min and L/S 5. pH in the reactor was controlled with a H_2SO_4/NaOH - pump and set to pH 4.5.Extraction efficiencies for different elements in this process step are shown in Figure 24. Percentages are determined by comparing the amounts of elements present in the leachate to the amounts in the solid sample before water washing. Concentrations of elements in leachates from this process step are presented in Table 10. Solid samples were analyzed using sodiumperoxide and ICP-OES technique. Liquid samples were also analyzed with ICP-OES.

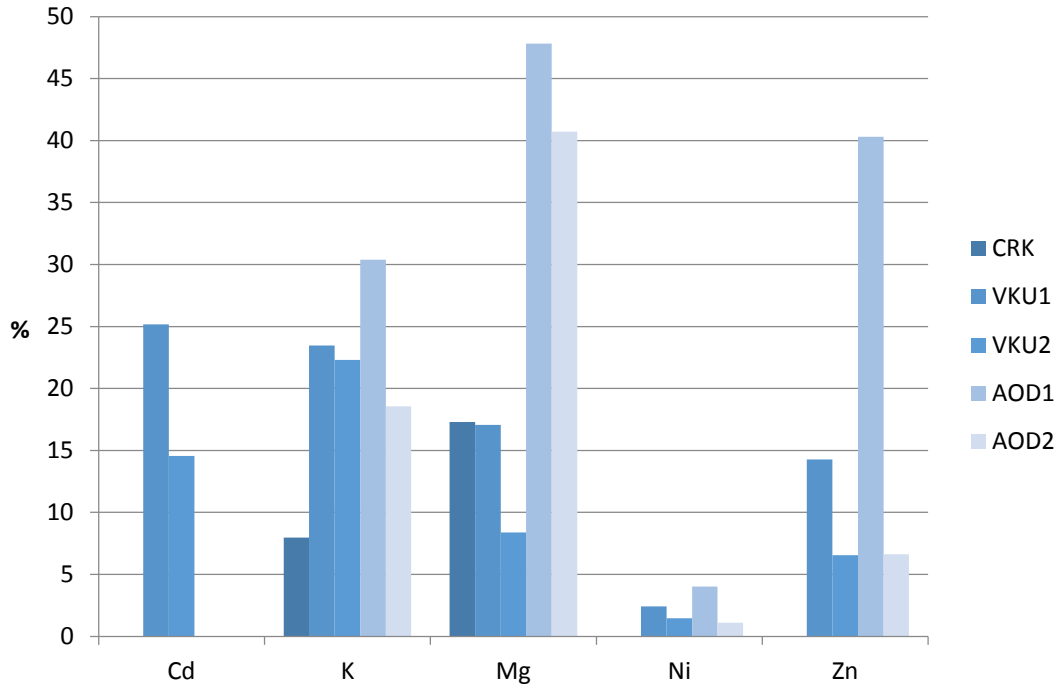

Figure 24. Extraction efficiencies (%) in first leaching.

Table 10. Concentration of elements (mg/l) in leachates from first leaching. Error estimate ±11 %.

	CRK	VKU1	VKU2	AOD1	AOD2
Cl	35.0	100	200	27,0	21.0
Ca	460	480	490	460	520
Cd	-	37.0	130	0,40	0,20
Cr	16.0	4,80	16.0	95.0	0,30
Fe	0,10	0,30	0,20	900	46.0
K	84.0	490	640	320	220
Mg	3860	1710	430	1770	2420
Mn	1,90	720	460	1020	390
Mo	1,20	0,20	0,30	0,12	25.0
Ni	0,01	110	120	66.0	78.0
Pb	-	-	-	6,50	-
S	5590	7310	4200	11750	6060
Zn	0,60	3770	1310	11100	1220
F	8,30	70	60	250	90

7.2.4 Second leaching

The duration of the second leaching step was 240 minutes and it was carried out in the same reactor as the first leaching, at 90 °C and L/S 5. Two different sulfuric acid concentrations were tested, 2 M and 6 M. When 6 M acid was used, some problems came up in filtering the slurries. The filters seemed to get blocked very fast after the slurries were poured out of the reactor. Small suction was therefore applied to enhance the filtration. For most samples, this procedure worked well. In the case of AOD2, a very wet sludge-like substance that could not be filtered was formed. In all cases, the filters were affected by the strong acid and became friable. After the solid residues were dried, it was observed that they still contained much more moisture than when more dilute acid was used. Also, when the temperature of the filtered leachate dropped, some elements started to precipitate from the solution.

Solid samples were analyzed using sodiumperoxide and ICP-OES technique. Liquid samples were also analyzed with ICP-OES. Extraction efficiencies for elements in this process step are presented separately for the two acid concentrations in Figures 25 and 26. Percentages are determined by comparing the amounts of elements present in the leachate to the amounts in the solid sample before water washing. Concentrations of elements in leachates from this step are presented in Tables 11 and 12. The precipitates of 6 M leachates that started to form in test tubes after sampling were analyzed and their composition is presented in Table 13.

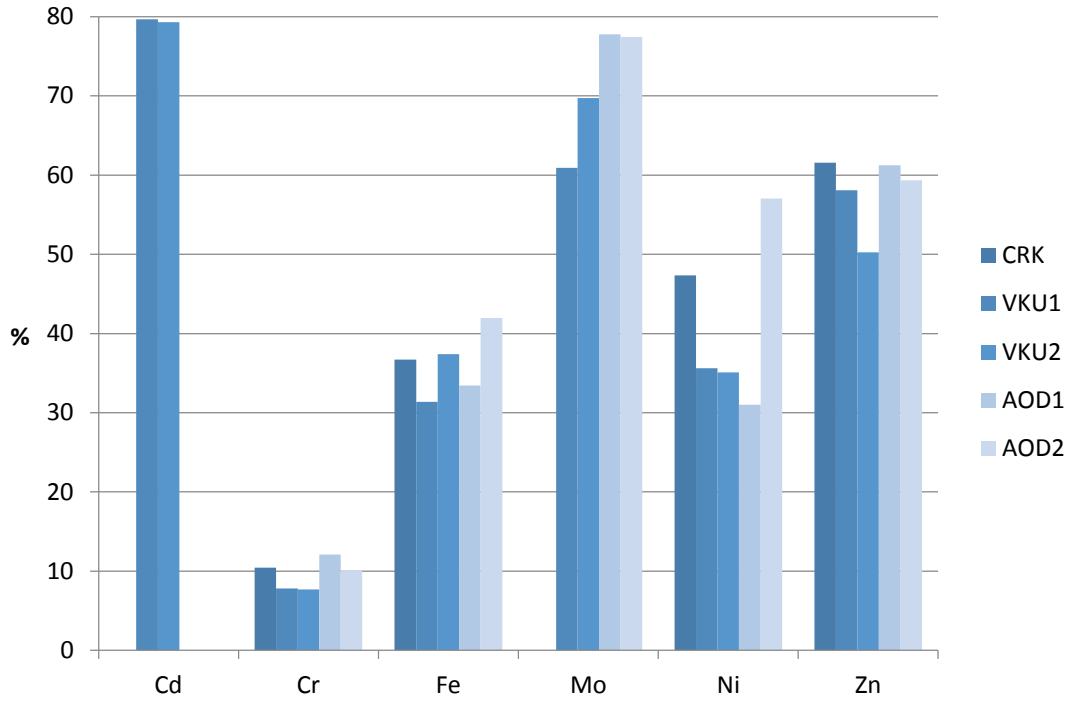

Figure 25. Extraction of elements (%) in second leaching (2M).

Table 11. Concentration of elements (mg/l) in leachate from second leaching (2M). Error estimate ±11 %.

	CRK	VKU1	VKU2	AOD1	AOD2
Ca	500	96800	610	450	250
Cd	0.60	-	590	0.5	1.70
Cr	5100	71400	3300	4870	5140
Fe	22530	105000	33550	56260	53390
K	170	1380	1150	160	220
Mg	18450	9890	2220	1100	6960
Mn	540	12200	5390	3910	8060
Mo	11.0	0	310	42.0	3750
Ni	140	7200	4060	900	7740
Pb	6.40	5950	12.0	9.70	8.20
S	90780	120000	101500	97490	124200
Zn	20660	24900	11070	13330	12250

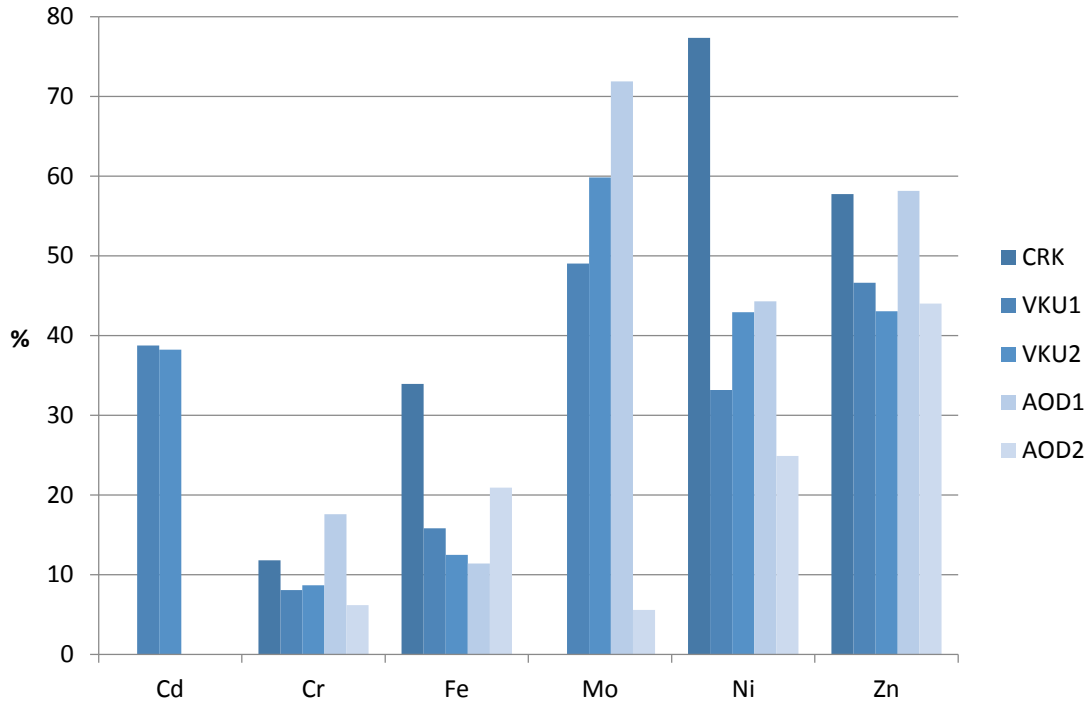

Figure 26. Extraction of elements (%) in second leaching (6M).

Table 12. Concentration of elements (mg/l) in leachate from second leaching (6M). Error estimate ±11 %.

	CRK	VKU1	VKU2	AOD1	AOD2
Ca	40.0	120	60.0	130	540
Cd	-	43.0	310	-	590
Cr	4540	3190	4150	9950	3510
Fe	10850	27060	4970	17340	34210
K	-	580	340	190	1180
Mg	14160	3440	1970	1410	2320
Mn	300	5580	3720	5910	5640
Mo	16.0	30.0	300	55.0	320
Ni	160	2250	5520	1860	4380
Pb	-	6.80	-	-	14.0
S	249400	238400	258900	236600	104400
Zn	14140	13130	9910	17600	11730

Table 13. Compositions (mg/kg) of precipitated material in leachates from second leaching (6M).

	CRK	VKU1	VKU2	AOD1	AOD2
Ca	1780 ± 360	1540 ± 310	1420 ± 290	1550 ± 310	1100 ± 220
Cd	-	30 ± 10	240 ± 70	-	-
Cr	4040 ± 1210	3240 ± 980	3610 ± 1080	3870 ± 1160	4180 ± 1260
Fe	59200 ± 11840	102000 ± 20400	109000 ± 21800	85100 ± 17020	61300 ± 12260
K	640 ± 380	-	2420 ± 1450	-	-
Mg	17900 ± 5370	4360 ± 1310	2850 ± 860	4660 ± 1400	5740 ± 1720
Mn	90 ± 200	4540 ± 910	5090 ± 1020	2240 ± 450	3540 ± 450
Mo	-	-	170 ± 70	1760 ± 710	2070 ± 830
Ni	130 ± 20	1750 ± 260	3500 ± 530	3980 ± 600	5640 ± 850
Pb	-	-	-	-	-
S	236000 ± 47200	247000 ± 49400	244000 ± 47800	239000 ± 47800	241000 ± 48200
Zn	20900 ± 4180	10300 ± 2060	9090 ± 1030	5140 ± 1580	7380 ± 1450

7.3 Concentrations in solid residues

Concentrations of the most interesting elements (Zn, Fe, Ni, Mo, Cr and S) in solid residues during the entire process are presented in Figures 27-38. Presentation is done separately for the two alternative process chains (i.e. second leaching done either with 2 M or 6 M sulfuric acid). Figures 27 and 28 were already presenter earlier in chapter 7.1.

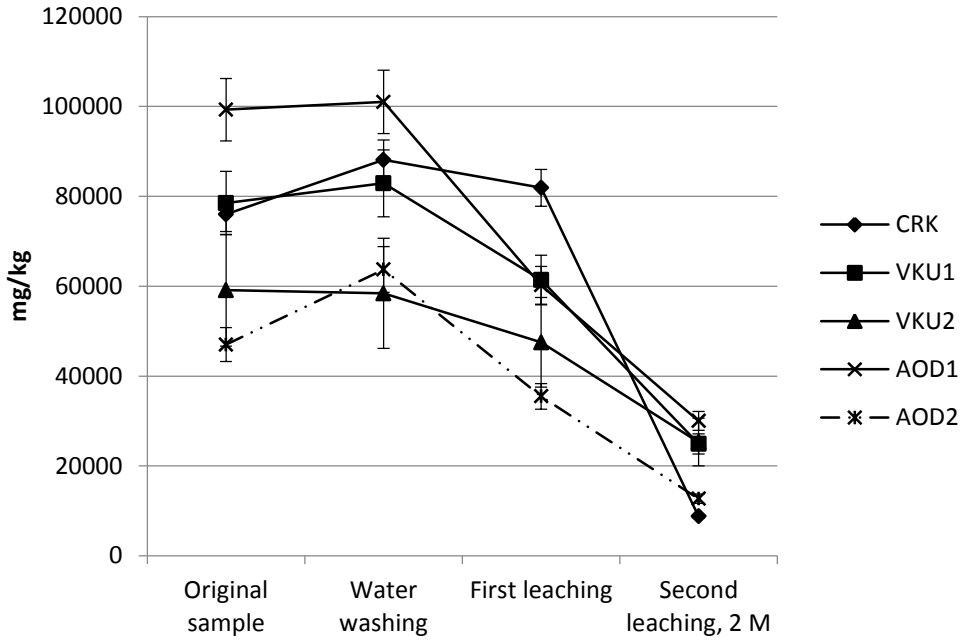

Figure 27. Zinc concentrations (mg/kg) in original samples and in solid residues after each process step. Second leaching was done using 2 M sulfuric acid.

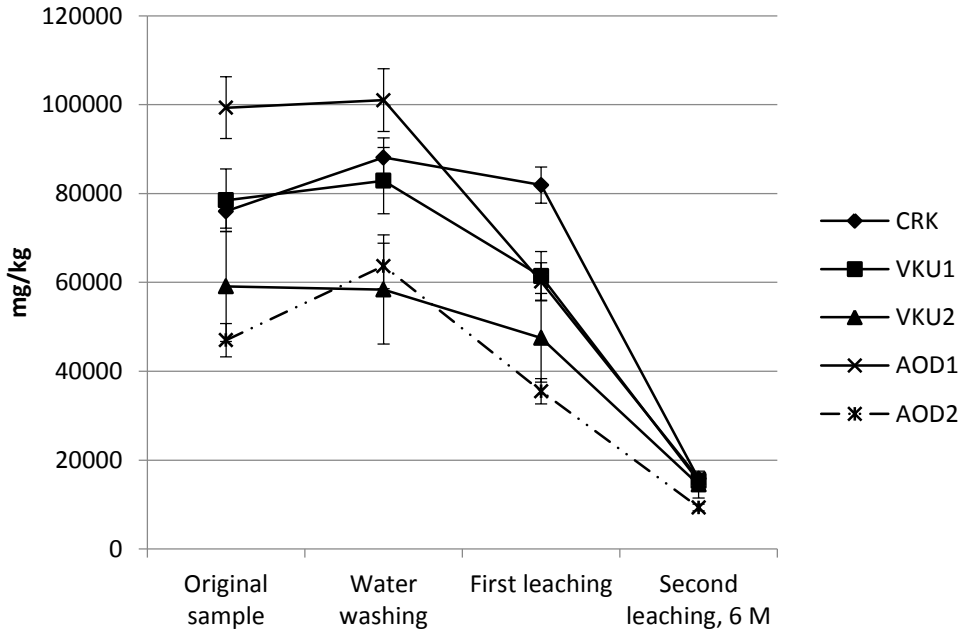

Figure 28. Zinc concentrations (mg/kg) in original samples and in solid residues after each process step. Second leaching was done using 6 M sulfuric acid.

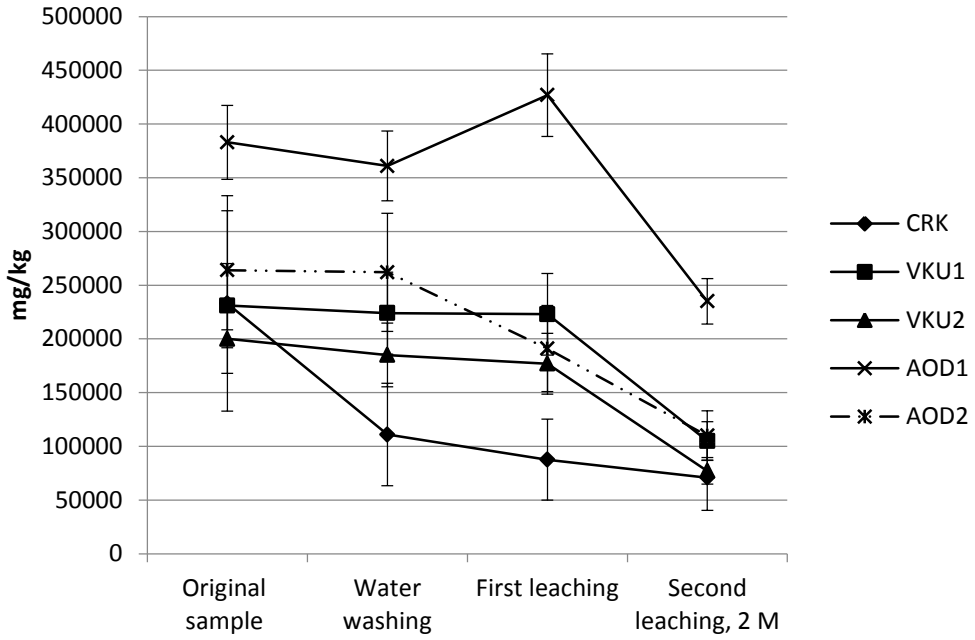

Figure 29. Iron concentrations (mg/kg) in original samples and in solid residues after each process step. Second leaching was done using 2 M sulfuric acid.

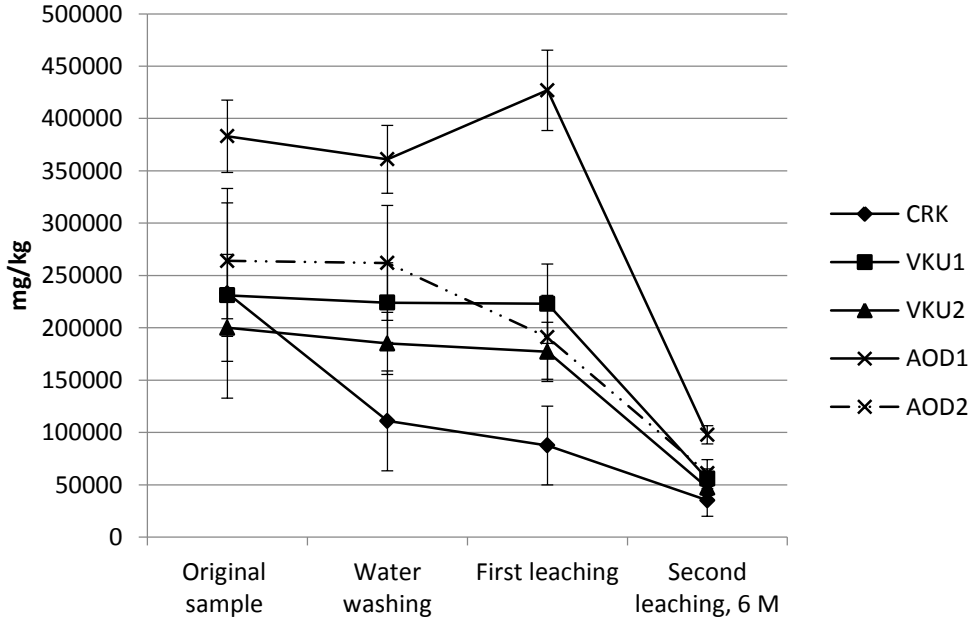

Figure 30. Iron concentrations (mg/kg) in original samples and in solid residues after each process step. Second leaching was done using 6 M sulfuric acid.

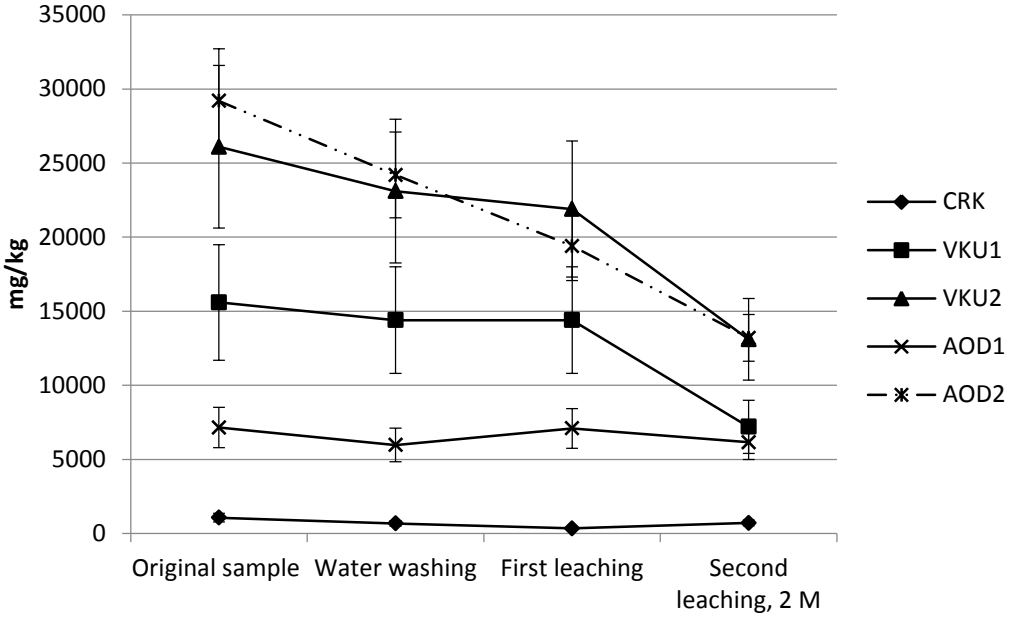

Figure 31. Nickel concentrations (mg/kg) in original samples and in solid residues after each process step. Second leaching was done using 2 M sulfuric acid.

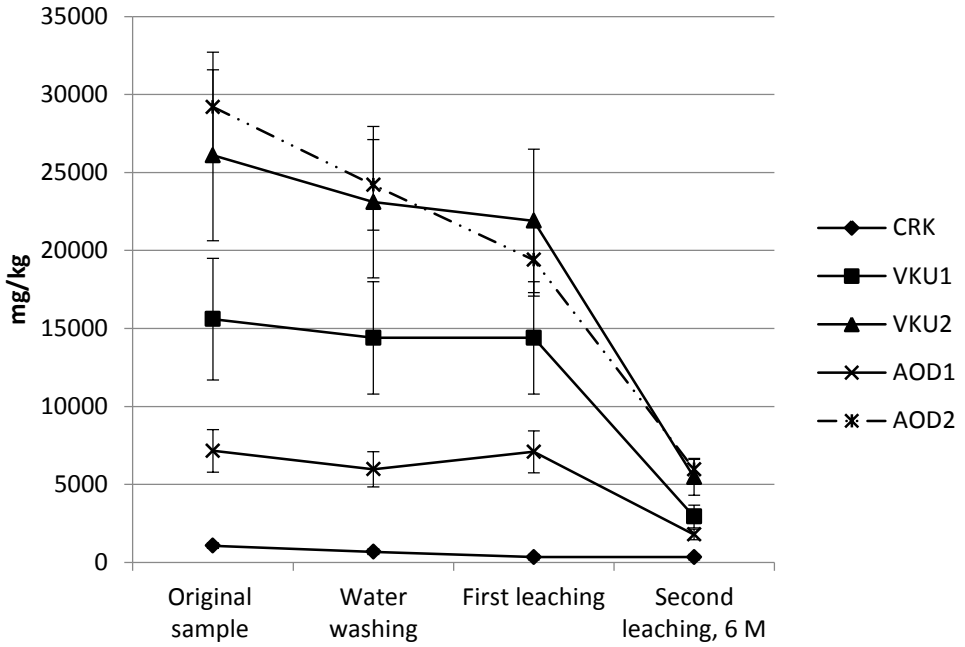

Figure 32. Nickel concentrations (mg/kg) in original samples and in solid residues after each process step. Second leaching was done using 6 M sulfuric acid.

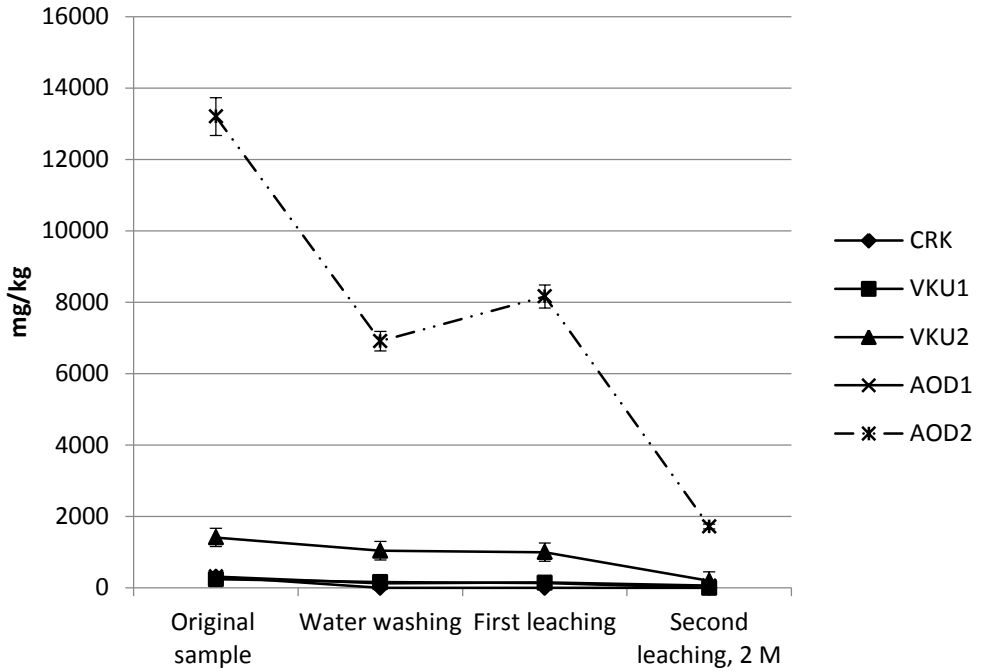

Figure 33. Molybdenum concentrations (mg/kg) in original samples and in solid residues after each process step. Second leaching was done using 2 M sulfuric acid.

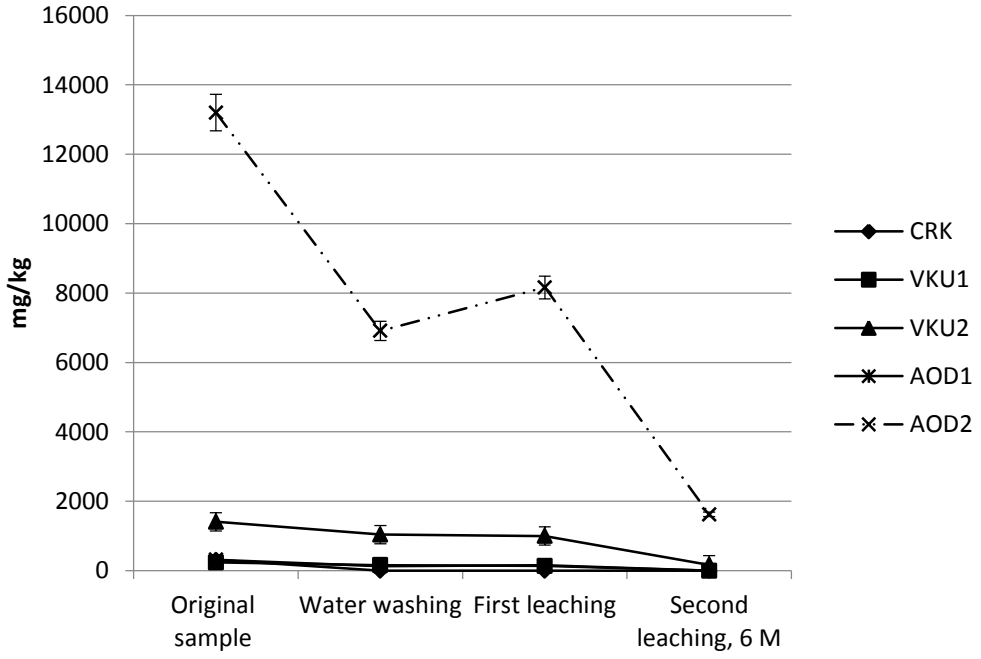

Figure 34. Molybdenum concentrations (mg/kg) in original samples and in solid residues after each process step. Second leaching was done using 6 M sulfuric acid.

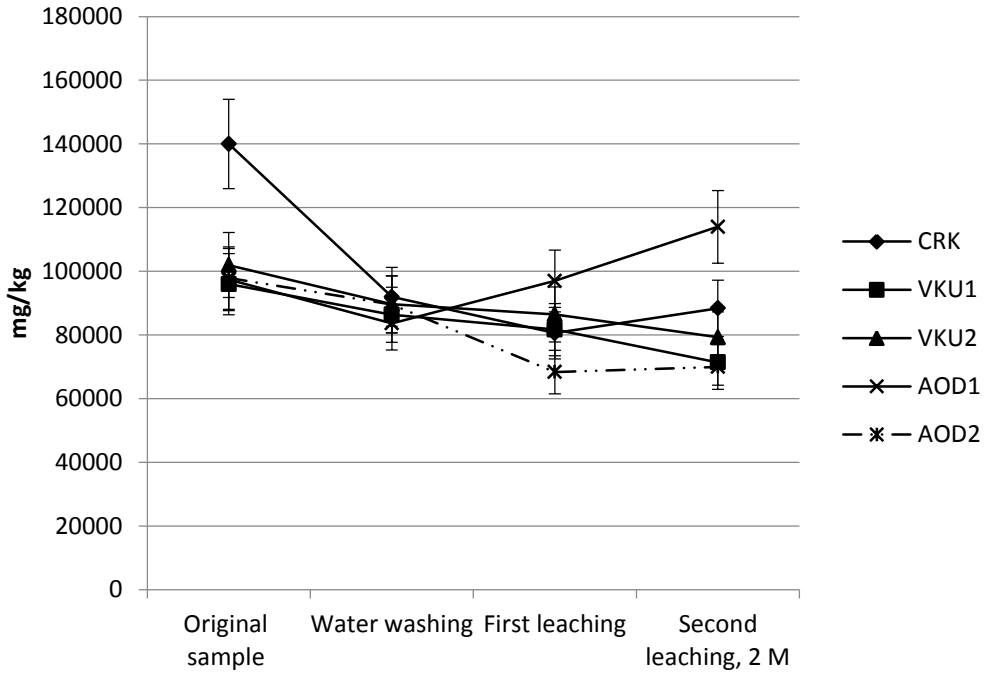

Figure 35. Chromium concentrations (mg/kg) in original samples and in solid residues after each process step. Second leaching was done using 2 M sulfuric acid.

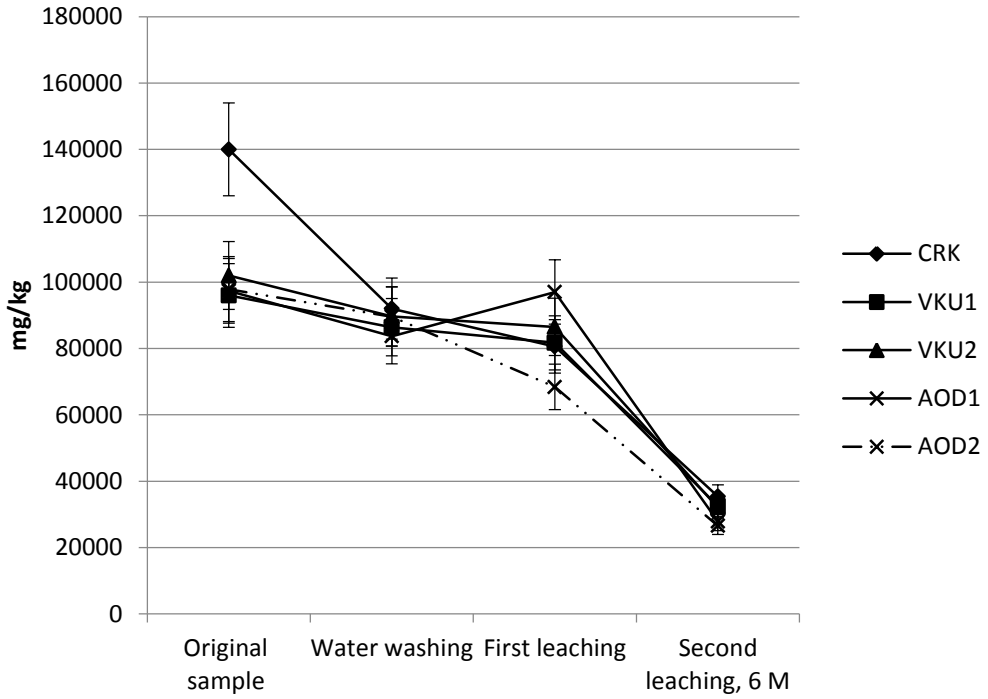

Figure 36. Chromium concentrations (mg/kg) in original samples and in solid residues after each process step. Second leaching was done using 6 M sulfuric acid.

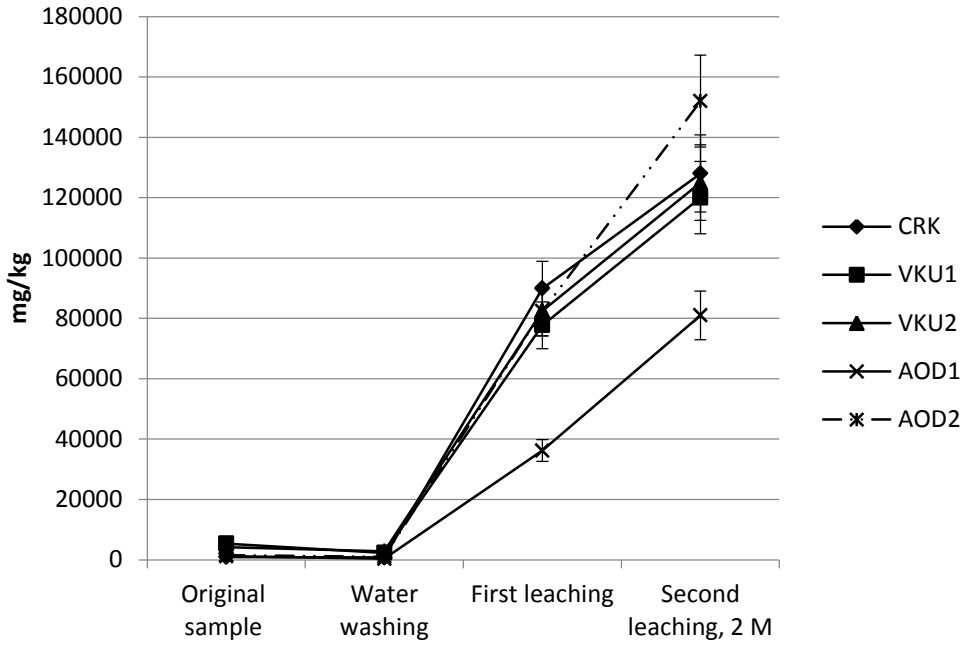

Figure 37. Sulfur concentrations (mg/kg) in original samples and in solid residues after each process step. Second leaching was done using 2 M sulfuric acid.

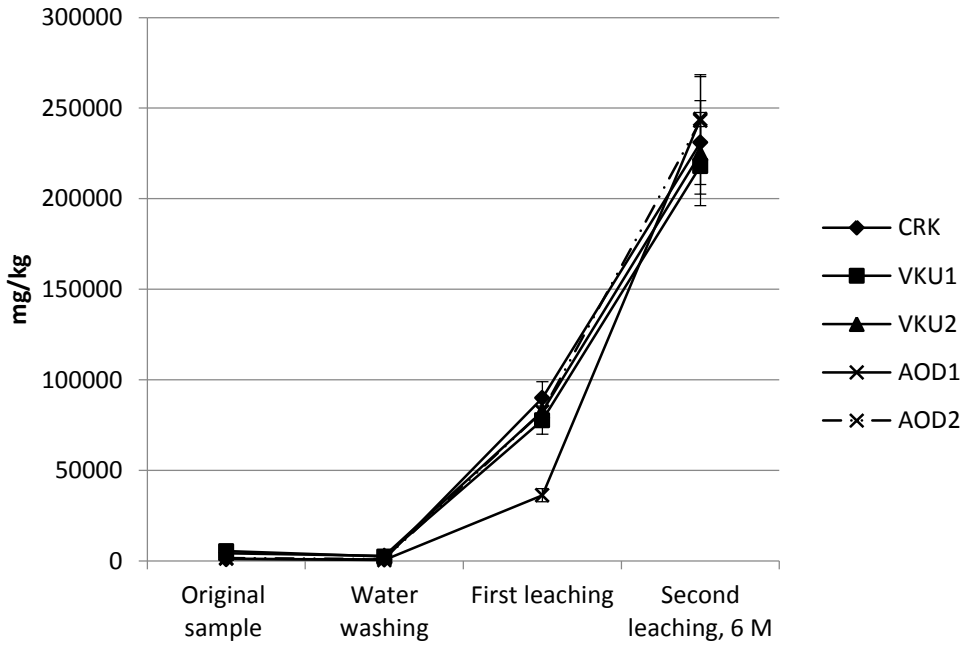

Figure 38. Sulfur concentrations (mg/kg) in original samples and in solid residues after each process step. Second leaching was done using 6 M sulfuric acid.

8 EVALUATION AND DISCUSSION

8.1 Error estimates

Solid samples were analyzed using ICP-OES technique either with agua regia or sodiumperoxide. Liquid samples were also analyzed with ICP-OES. The analyzing laboratory, Labtium Oy, reported 25 % an 12 % average uncertainity in ICP analysis to solid and liquid samples, respectively. Another estimate of error was obtained by comparing three different analysis that were done for the original dust samples (Table 14). These estimates give a better impression of the error that is related to ICP analysis as well as sampling and they are used for solid samples. For liquid samples, estimates from Labtium Oy are used. Additional error to the results comes from the heterogenity of samples. Sampling and sample preparation were done manually and their accuracy threfore limited.

Table 14. Standard deviations (%) for different samples and elements. Values were obtained by comparing three analysis of original samples.

	CRK	VKU1	VKU2	AOD1	AOD2
Ca	9	4	4	6	5
Cl	10	10	10	10	10
Cr	10	10	10	10	10
Fe	43	17	16	9	12
K	68	5	2	10	6
Mg	6	11	22	4	3
Mn	52	16	27	20	31
Mo	89	3	5	14	4
Ni	27	25	21	19	12
Zn	5	9	21	7	8

8.2 Water washing

Results from this process step were satisfying and in correlation with previous studies [Bruckard *et al.* 2005, Chen *et al.* 2011] even though maximum extraction rates were not reached. 77-93 % chloride, 11-63 % potassium and by 3-10 % calcium was extracted during water washing. Some differences were noticed compared to results from preliminary experiments. The yield of potassium was lower than in the preliminary experiments for both samples. Chloride and calcium removal were the same as in preliminary tests. For VKU1, VKU2, AOD1 and AOD2 molybdenum was leached; highest some 30 % in VKU1 and AOD2 which also had the highest Mo content. The leaching of Mo was probably due to presence of MoO or other molybdenum oxides [Ma *et al.* 2006, Nyirenda 1991]. As desired, the extraction of zinc in this step was negligent for all dust samples.

Molybdenum was detected in the leachates, which in some cases might have economic value: the leachate from AOD2, for example, contained 996 mg /l of molybdenum. The leachates also contained chromium that was present from 15.7 to 214 mg/l. Chromium concentrations exceed the 5 mg /l limit values that are stated in EU and US legislation [Environmental permit for Tornio Works, Leclerc *et al.* 2003] and therefore the leachates have to be treated before discharging. Bruckard *et al.*, for instance, mention that heavy metals could be removed by simple sodium sulfide treatment [Bruckard *et al.* 2005].

Because of two different analysis methods were used by the analysing laboratory, yields for preliminary experiments and actual experiments were defined differently. Yields in preliminary washing were calculated from the amounts of elements in the original samples and solid residues, where as yields for actual tests were calculated from amounts of elements in the original samples and leachates. This difference might have affected the comparability of the results.

8.3 First leaching

Results from first leaching were not entirely what were expected. Zinc removal of only 0-40 % was achieved: CRK 0 %, VKU1 14 %, VKU2 7 %, AOD1 40 % and AOD2 7 %. Additionally, the overall leaching of other elements was low, except for Cl, K, Ca and Mg.

Theoretically, zinc oxides would have been leached during this process step and yield percentages would have been higher. Havlik *et al.* [Havlik *et al.* 2006] for instance reported zinc recoveries of more than 60 % in leaching with 0.5 M sulfuric acid, using similar parameters, except for higher L/S 12.5. Kekki *et al.* [Kekki *et al.* 2012] also reached higher leaching rates to the same samples that were studied in this thesis. The parameters they used were similar, except for longer time (120 min) and higher L/S 10.

The reason for poor leaching might have been a malfunction in the reactor´s pH control system. The system was supposed to measure the pH in the reactor and keep it below pH 4.5 by pumping either additional sulfuric acid or sodium hydroxide to the reactor. Some air bubbles were detected in the pump´s tubes that maybe affected the pumping rate. From the measured time- pH diagram (Figure 39) it can be seen that in most cases pH values rose above 4.5 or were very close to that. In the case of CRK, the desired pH level was never even reached, which can explain the exceptionally low zinc leaching. It could be possible that zinc removal could be enhanced by increasing the L/S ratio. To evaluate the effect of pH, second tests without pH control were done for two samples (VKU2 and AOD1). Changes in pH during the tests are shown in Figure 40.

Another interpretation of poor leaching is that 0.5 M acid is not strong enough to leach zinc oxides from the dusts (except in the case of AOD1). All that would have been soluble in this step would then have been leached already in the previous water washing step. Because the function of pH control was left unclear, this process step is recommended to be tested again in order to draw stronger conclusions.

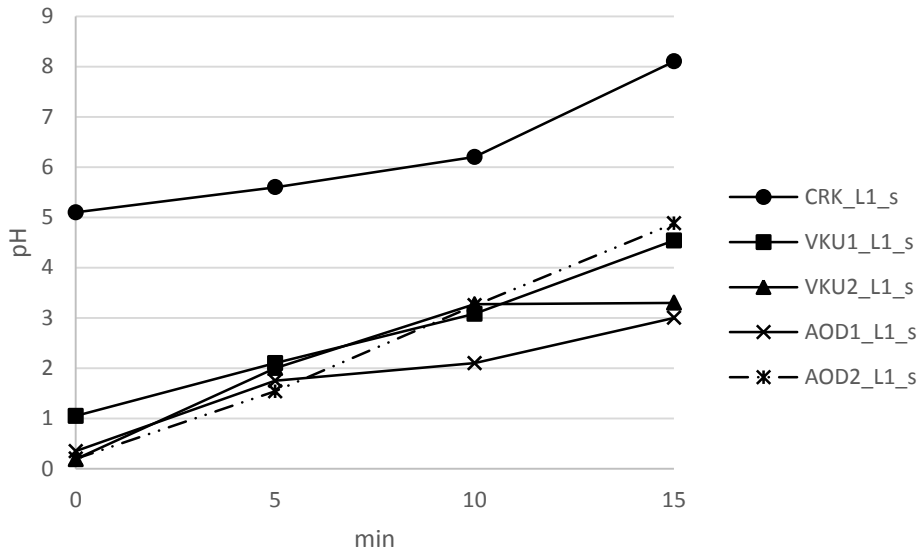

Figure 39. Time- pH diagram from first leaching.

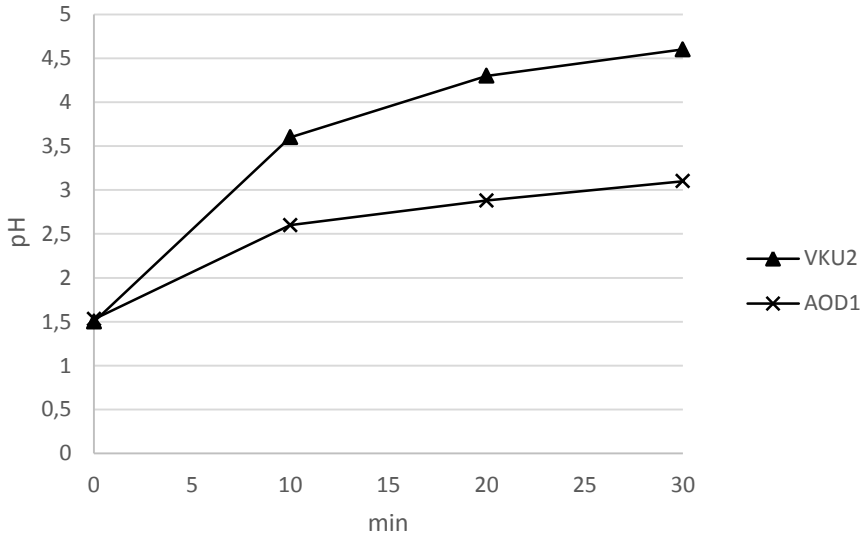

Figure 40. Changes in pH during re- runs of first leaching (only for VKU2 and AOD1).

By comparing Figures 39 and 40, it can be seen that in the case of VKU2, pH values rose faster without pH control. Same kind of behavior was not observed for AOD1. Zinc recovery without pH control was 9 % for VKU2 and 14 % for AOD1. The relatively low zinc recovery for AOD1 (14 % vs. 40 %) cannot be explained by pH but

has to be dependent on other factors in the experiment or analysis or either on the sample´s characteristics.

The leachates from this process step did not contain much zinc, iron or alloying elements. Highest zinc concentration in this step was achieved for AOD1 (11100 mg/l). The same leachate contained also the highest concentration of iron (900 mg/l). Iron and other impurities have to be removed by solution purification methods, before the leachate could be used in electrolytic zinc production. According to Herrero *et al.* [Herrero *et al.* 2010] electrolytes that could be used in zinc production should contain 50-70 g/l zinc. Concentration limits for impurities were presented in Table 10.

8.4 Second leaching

For both acid concentrations, zinc removal in this step was between 43-61 % but the highest percentages for all samples were reached when leaching was done using 2 M acid: CRK 62 %, VKU1 58 %, VKU2 50%, AOD1 61 % and AOD2 59 %. Compared with results that have been reported in other studies, these percentages were rather low. Langova *et al.* [Langova *et al.* 2007] for instance reported almost 100 % zinc extraction in 3 M sulfuric acid, 80 °C, L/S 5 and 6 hours. The dusts mineralogy is of course unique in every case and determines how different elements are leached. Kekki *et al.* [Kekki *et al.* 2012], who studied some of the same samples, achieved to leach 65-100 % of zinc from the dusts with 1.5, M sulfuric acid, 90 °C, L/S 10 and 2 hours.

Nevertheless, it should be noted that crystalline sulphates started to form in all 6 M leachates. This precipitation decreased the zinc concentration in the leachates, so the concentrations in 6 M solutions were initially higher that the analysis reveals. It was practically impossible to measure the weights of the precipitates to evaluate the loss of elements from the solution. The yields for 6 M leaching should be viewed together with the precipitate analysis in order to get a better picture of total leaching.

Changes in pH and zinc concentration in the leachate during the second leaching are presented in Figures 41- 44, first for 2 M acid and then for 6 M acid.

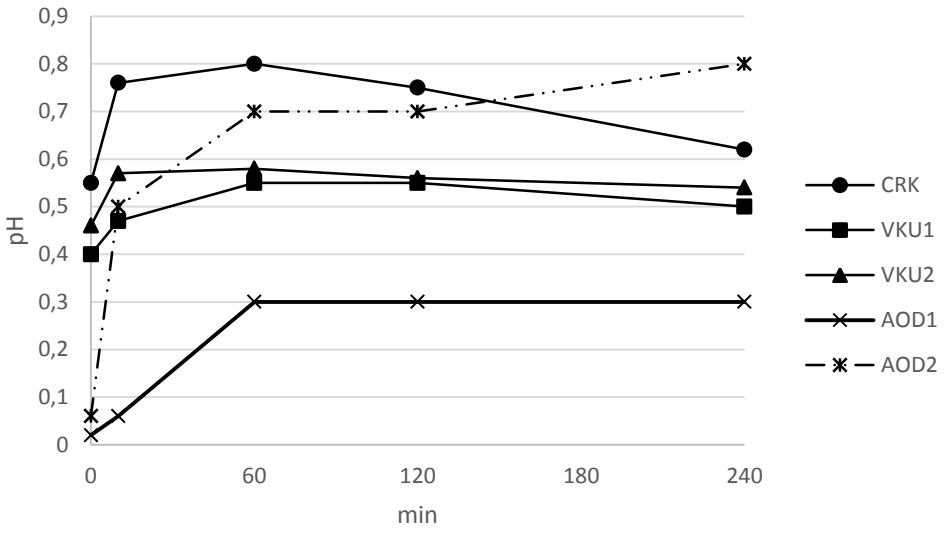

Figure 41. Time- pH diagram from second leaching (2 M).

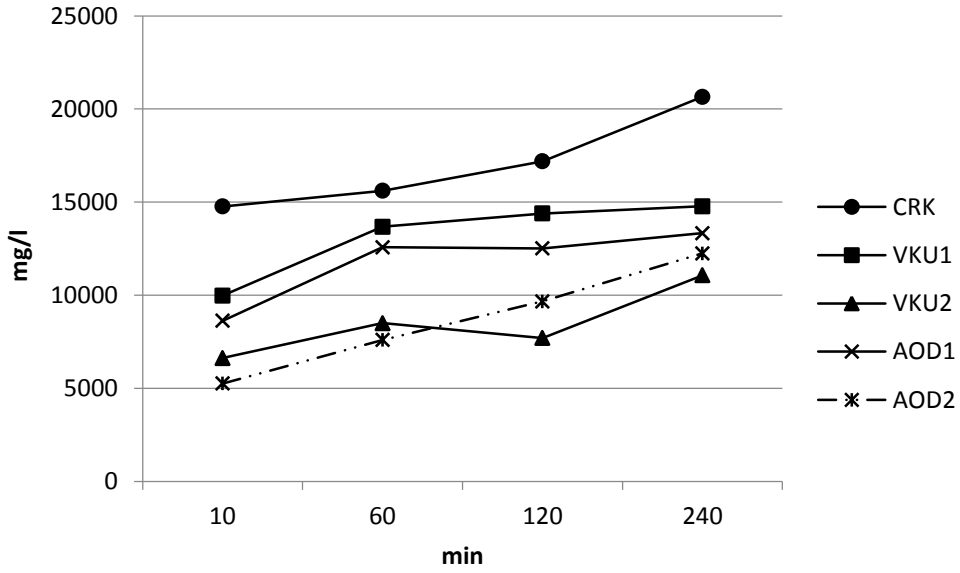

Figure 42. Zinc concentration in leachate during second leaching (2 M).

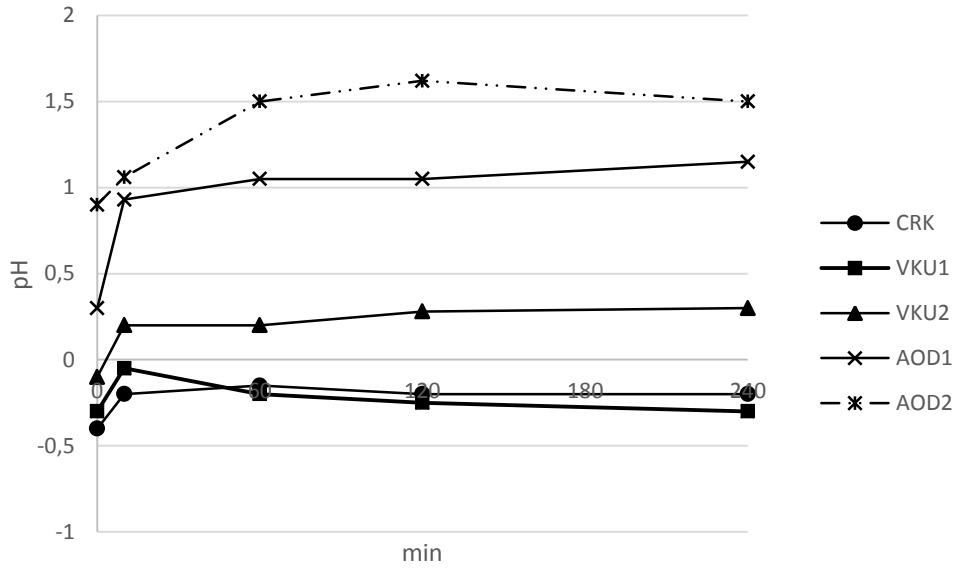

Figure 43. Time- pH diagram from second leaching (6 M).

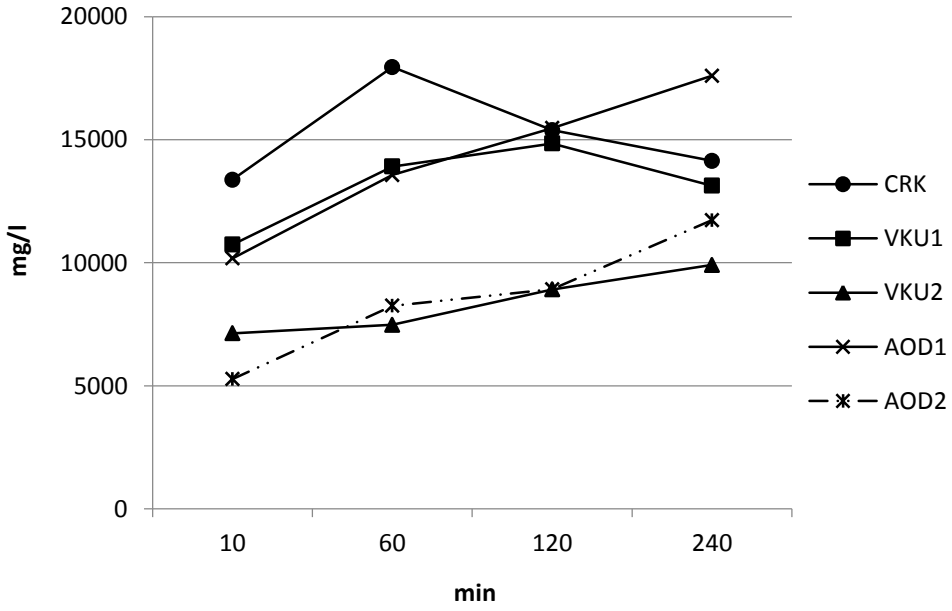

Figure 44. Zinc concentration in leachate during second leaching (6 M).

By comparing Figures 41 and 43, it can be seen that in the case of AOD2 pH values rose higher when leaching was done with 6 M acid. This has to be related to leaching of certain elements but it not clear which ones. When CRK was leached with 6 M acid, zinc concentration in leachate started to decrease after 60 minutes. The pH of the solution must have exceeded a limit where zinc started to precipitate (see Figure 9 for E-pH diagram of the Zn-Fe-H_2O system).

Regarding the solid residues from leaching with 2 M or 6 M acid, a steep increase in sulfur content was observed (see Figures 37 and 38). High sulfur concentration will be a problem as sulfur has to be removed before the residues can be fed back to steel making process. Furthermore, sulfuric concentrations in all samples exceed the limits that are applied in Finnish landfill sites (see Table 3). Limit values for heavy metals are also exceeded. The rise in sulfur concentration is due to formation of crystalline sulphates, and the only way to remove them would probably be washing the residues with hot water. This would impair the process as it results in higher water and energy consumption.

The yields for Cr, Ni and Mo in this step were 30- 66 %, 10 % and 5- 77 %. The dust´s mineralogy is thought to have the most effect on their leaching. A leachability study by Laforest *et al.* reports that Cr and Ni were found to be tightly bound to iron or chromium oxides or spinel group minerals. Oxides are more easily soluble than spinels. Spinels are soluble only in concentrated acid so the removal of Cr and Ni could be expected only in this process step as 2 M or 6 M were used [Laforest *et al.* 2006]. Molybdenum on the other hand is found to be present as oxides and was therefore leached also in the water washing step [Ma *et al.* 2006, Nyirenda 1991].

9 CONCLUSIONS AND RECOMMENDATIONS

Based on experimental work, the following answers can be given to answer three research questions:

1. Can a multistage leaching process be used in breaking franklinite and can it enhance zinc removal from flue dusts?

   The process that was tested (see Figure 46) contained two steps where the dust were leached with sulfuric acid: first leaching was done with 0.5 M acid, 15 min, 90 °C, L/S 5 and the second one with 2 M or 6 M acid, 240 min, 90 °C, L/S 5. Yields in the first leaching were relatively low: CRK 0 %, VKU1 14 %, VKU2 7 %, AOD1 40 % and AOD2 7 %. Highest zinc removal rates in the second leaching were reached with 2 M acid: CRK 62 %, VKU1 58 %, VKU2 50%, AOD1 61 % and AOD2 59%. On these basis, multistage leaching doesn´t seem to be advantageous to single phased leaching with 1.5 M sulfuric acid for example (except for AOD1). Because of potential malfunction in the pH control system, repetition of this process step is recommended in order to draw more secure conclusions.

2. How do Ni, Cr and Mo behave during the process?

   Nickel was not leached during the first two process steps. Yields in water washing were practically 0 % and in the first leaching only 0-4 %. In the second leaching step yields were between 30-60 %. Chromium was not leached at all during the first two steps and yields in the second leaching step were only around 10 %. 15-33 % of molybdenum leached already during the water washing step, but its removal was minimal during the first leaching. In the second leaching step molybdenum yields were 5-77 %. The dust´s mineralogy is thought to have the most effect on the leaching of Ni, Cr and Mo during the process.

3. Can halides be removed from the dusts by water washing pre- treatment?

   80-90 % chloride, 30-60 % potassium and 3-10 % calcium were removed when washing was done for 60 minutes at ambient temperature and L/S 5. Water washing can be used in removing most of the halides from the dusts, the process was fairly simple and the slurries were easy to filter.

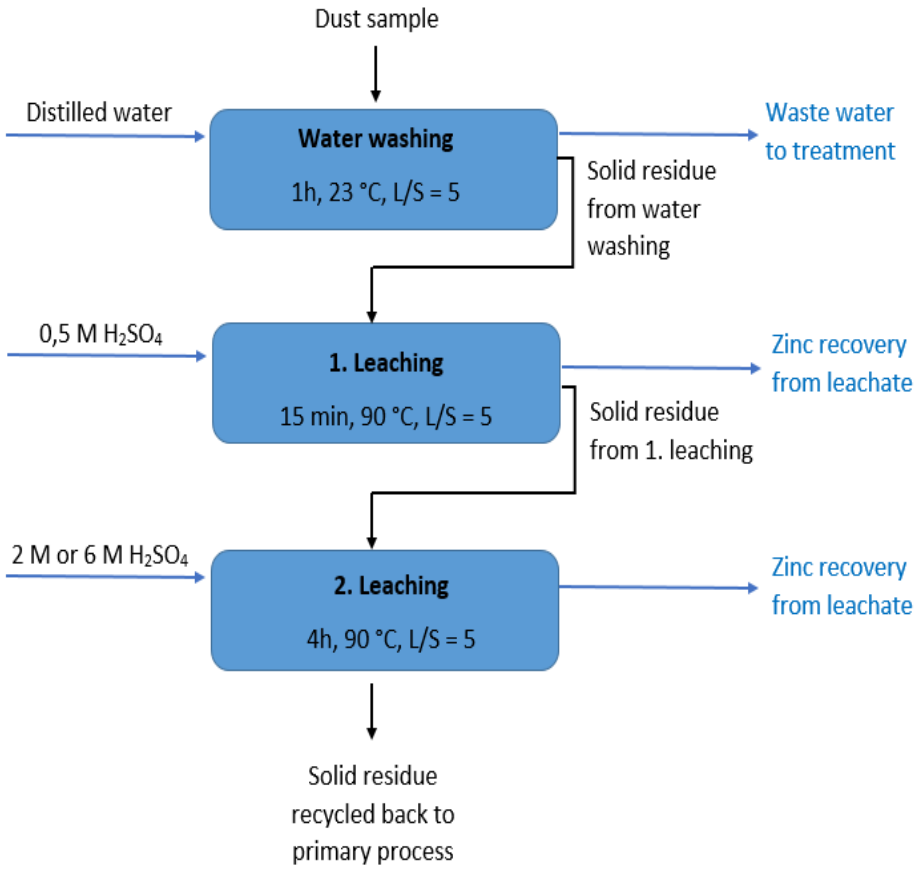

Figure 45. Flow chart of the tested multistage process.

11 REFERENCES

Antrekowitsch, J., Steinlechner, S., & Schneeberger, G. (2010). Evaluation and recycling potential of different zinc containing residues from metallurgical industry. TMS Lead-Zinc 2010: pp. 851-859.

Arslan, C. & Arslan, F. (2003). Thermodynamical Review of Jarosite and Goethite Stability Regions at 25 and 95 °C. Turkish J. Eng. Env. Sci. 27: pp. 45-52.

Aromaa, J. (1990). Hydrometallurgian perusteet – teoriaa ja prosessiesimerkkejä. Raportti TKK-V-KORR-9. Teknillinen Korkeakoulu, Otaniemi. 134 p.

Bruckard, W.J., Davey, K.J., Rodopoulos, T., Woodcock, J.T. & Italiano, L. (2005). Water leaching and magnetic separation for decreasing the chloride level and upgrading the zinc content of EAF steelmaking bag house dusts. International Journal of Mineral Processing 75: pp. 1-20.

Burkin, A.R. (2001). Chemical Hydrometallurgy, Theory and Principles. Imperial College Press. 414 p.

Caravaca, C., Cobo, A., & Alguacil, F.J. (1994). Considerations about the recycling of EAF flue dusts as source for the recovery of valuable metals by hydrometallurgical processes. Resources, Conservation and Recycling 10 (1-2): pp. 35-41.

Chen, W., Shen, Y., Tsai, M. & Chang, F. (2011). Removal of chloride from electric arc furnace dust. Journal of Hazardous Materials 190: pp. 639-644.

Cruelles, M. Roca, A. & Nunez, C. (1992). Electric arc furnace flue dusts: characterization and leaching with sulphuric acid. Hydrometallurgy 31(3): pp. 213-231.

Denton, G. M. (2005). EAF Stainless Steel Dust Processing. Sustainable developments in metals processing, Melbourne, Australia.

Dutra, A.J.B. (2006). Alkaline leaching of zinc from electric arc furnace steel dust. Minerals Engineering 19 (5): pp. 478-486.

Fujii, H., Nagaiwa, T., Kusuno, H. & Malm, S. (2005). How to quantify the environmental profile of stainless steel. SETAC North America 26: th Annual Meeting.

Goff, T.J. & Denton, G.M. (2004). Direct smelting of stainless steel plant dusts. Tenth International Ferroalloys Congress, Cape Town, South Africa.

Guezennec, A, Huber, J., Patisson, F. Sessiecq, P., Birat, J & Ablitzer, D. (2005). Dust formation in Electric Arc Furnace: Birth of the particles. Powder Technology 157: pp. 2-11.

Havlik, T., Souza, E., Vidor, B., Bernardes, A.M., Schneider, I.A.H. & Miskufova, A. (2006). Hydrometallurgical processing of carbon steel EAF dust. Journal of Hazardous Material B135: pp. 311-318.

Havlík, T., Miskufova, A., Kukuruyga, F., Orac, D. Takacova, Z. & Laubertova, M. (2010). Scientific research and analysis of steel making dusts and sludges. Kosice, Slovakia: Technical university of Košice.

Heikkinen, E.P. (2012). Sinkin valmistus: Metallurgiset prosessit ja niiden mallinnus. Presentation 20.9.2012. University of Oulu.

Herlitz, H.G. (1982). The plasmadust process for recovery of metals from waste oxides. Resources and Conservation 9: pp. 191- 198.

Herrero, D., Arias, P.L., Güemez, B., Barrio, V.L., Cambra, J.F. & Requie, J. (2010). Minerals Engineering 23: pp. 511-517.

Hoang Trung, Z. Kukurugya, F., Takacova, Z., Orac, D., Laubertova, M. Miskufova, A. & Havlik, T. (2011). Acidic leaching both of zinc and iron from basic oxygen furnace sludge. Journal of Hazardous Material 192: pp. 1100-1107.

Jha, M.K., Kumar, V. & Singh, R.J. (2001). Review of hydrometallurgical recovery of zinc from industrial wastes. Resources, Conservation and Recycling 33 (1): pp. 1-22.

Kekki, A., Aromaa, J. & Forsen, O. (2011). Leaching and Recovery of Stainless Steel Production Dusts in Acidic Media. EMC 2011.

Kekki, A., Aromaa, J. & Forsen, O. (2012). Leaching Characteristics of EAF and AOD Stainless Steel Production Dusts. Physiochemical Problems of Mineral Processings 48: pp. 599-606.

Kelebek, S., Yoruk, S., & Davis, B. (2004). Characterization of basic oxygen furnace dust and zinc removal by acid leaching. Minerals Engineering 17: pp. 285- 291.

Kemperman, D. (2010). Metallurgical processing of zinc-bearing residues. Delft University of Technology, Department of Geotechnology.

Laforest, G. & Duchesne, J. (2006). Characterization and leachability of electric arc furnace dust made from remelting of stainless steel. Journal of Hazardous Materials B135: pp. 156-164.

Langova, S., Riplova, J. & Vallova, S. (2007). Atmospheric leaching of steel-making wastes and the precipitation of goethite from the ferric sulphate solution. Hydrometallurgy 87: pp. 157-162.

Leclerc, N., Meux, E. & Lecuire, J. (2003). Hydrometallurgical extraction of zinc from zinc ferrites. Hydrometallurgy 70: pp. 175-183.

Li, C., & Tsai, M. (1992). Mechanism of Spinel Ferrite Dust Formation in Electric Arc Furnace Steelmaking. ISIJ International 33 (2),: pp. 284-290.

Ma, G. & Garbers-Craig, A.M. (2006). Cr(VI) containing electric furnace dusts and filter cake from a stainless steel waste treatment plant: Part 1 - Characteristics and microstructure. Ironmaking & Steelmaking 33(3): pp. 229-237.

Maccagni, M. & Nielsen, J. (2010). Zinc recovery from secondaries and wastes. Lead-Zinc 2010: pp.165-175.

Machado, J., Brehm, F.A., Mendes Moraes, C.A., dos Santos, C.A., Faria Vilela, A.C. & Marimon da Cunha, J.B. (2006). Chemical, physical, structural and morphological characterization of the electric arc furnace dust. Journal of Hazardous Materials B136: pp. 953-960.

Majuste, D. & Mansur, M.B. (2008). Acid leaching of the fine fraction of the AOD-L sludge generated by the stainless steel making process in order to recover chromium, nickel and iron. Hydrometallurgy 2008: Proceedings of the Sixth International Symposium. pp. 183-191.

Majuste, D. & Mansur, M.B. (2009). Leaching of the fine fraction of the argon oxygen decarburization with lance (AOD-L) sludge for the preferential removal of iron. Journal of Hazardous Materials 162(1): pp. 356-364

Makkonen, H.T. & Angerman, M. (2010). Ruostumattoman teräksen valmistuksessa Outokumpu OYJ:n Tornion tehtaalla syntyvien pölyjen sekä regenerointisuolan ja neutralointisakan karakterisointi. University of Oulu, Department of process and environmental engineering.

Meurer, U. & Butenbach, S. (2001). Recycling Processes for Residues of the Steel Industry - Treatment of Stainless Steel Production Residues and Alloy Recycling. EMC 2001, Friedrichshafen, Germany. pp. 239- 258.

Nakamura, T., Shibata, E., Takasu, T. & Itou, H. (2008). Basic Consideration on EAF Dust Treatment Using Hydrometallurgical Processes. Resources Processing (55): pp. 144-148.

Nasmyth, M. & Cooper, G. (2010). Feed materials and process options. Lead-Zinc 2010: pp. 291-306.

Nyirenda, R. L. (1991). The processing of steelmaking flue-dust: A review. Minerals Engineering 4 (7-11): 1003-1025.

Oustadakis, P., Tsakiridis, P.E., Katsiapi, A. & Agatzini-leonardou, S. (2010). Hydrometallurgical process for zinc recovery from elecrtic arc furnace dust (EAFD). Part I: Characterization and leaching by diluted sulphuric acid. Journal of Hazardous Materials 179: pp. 1-7-

Palencia, I., Romero, R., Iglesias, N. & Carranza, F. (1999). Recycling EAF Dust Leaching Residue to the Furnace. A Simulation Study. Journal of Materials, August 1999: pp. 28- 32.

Rao, S.R. (2006). Chapter 8: Metallurgical slags dusts and fumes. Waste Management Series, Volume 7, Elsevier: pp.269-327.

Reck, B.K., Chambon, M., Hashimoto, S. & Graedel, T.E. (2010). Global Stainless Steel Cycle Exemplifies China's Rise to Metal Dominance. Environ. Sci. Technol. 44: pp. 3940-3946.

Reuter, M.A., Boin, U.M.J., van Schaik, A., Verhoef, E., Heiskanen, K., Yang, Y. & Georgalli, G. (2005). Metrics of Material and Metal Ecology, Harmonizing the Resource, Technology and Environmental Cycles, Elsevier Science & Technology. 720 p.

Reyad, A.S. (2010). Hydrometallurgical extraction of zinc from Jordanian electric arc furnace dust. Hydrometallurgy 104: pp.61-65.

Ruetten, J. (2010). Different Ways of Using Waelz Oxide - Overview and Evaluation. Lead-Zinc 2010: pp.841-849.

Schumacher, K. & Sands, R.D. (2007). Where are the industrial technologies in energy- economy models? An innovative CGE approach for steel production in Germany. Energy Economics 29: pp. 799-825.

Sofilic, T., Rastovcan-Mioc, A., Cerjan-Stefanovic, S., Novosel-Radovic, V. & Jenko, M. (2004). Characterization of steel mill electric-arc furnace dust. Journal of Hazardous Materials B109 (1-3): pp.59-70.

Sohn, H.Y. (2001). Hydrometallurgical Principles. Encyclopedia of Materials: Science and Technology (Second Edition). Oxford, Elsevier: pp. 3976-3981.

Stefanova, A., Aromaa, J. & Forsen, O. (2013). Alkaline leaching of zinc from argon oxygen decarbonization dust from stainless steel production. Physiochemical Problems in Minerals Processing 49(1). pp. 37-46.

Stefanova, A. & Aromaa, J. (2012). Alkaline leaching of iron and steelmaking dust. Aalto University publication series, Science + Technology 1/2012.

Stegemann, J.A., Amitava, R., Caldwell, R.J., Schilling, P.J. & Tittsworth, R. (2000). Understanding Environmental Leachability of Electric Arc Furnace Dust. Journal of Environmental Engineering, February 2000: pp.112-120.

Xia, D.K., & Pickles, C.A. (2000). Microwave caustic leaching of electric arc furnace dust. Minerals Engineering 13(1): 79-94. Canadian Metallurgical Quarterly 38(3): pp. 175-186.

Zunkel, P. E. (2001). Recovering Zinc and Lead from Electric Arc Furnace Dust: A 2001 Processing and Technology Status Update. EMC 2001, Friedrichshafen, Germany.

Environmental permit for Tornio Works. (2012). Aluehallintoviraston lupapäätös nro 83/12/1 / dnro PSAVI/57/04.08/2010.

Industrial Emissions Directive 2010/75/EU. European Commission, Best Available Techniques (BAT) Reference Document for Iron and Steel Production.

Valtioneuvoston asetus 331/2013. Cited 30.7.2013. Available at: http://www.finlex.fi/fi/laki/alkup/2013/20130331

Ympäristöministeriön asetus 1129/2001. Cited 30.7.2013. Available at: http://www.finlex.fi/fi/laki/smur/2001/20011129 (30.7.2013).

London Metals Exchange. Cited 30.4.2013. Available at: http://www.lme.com/metals/reports/averages/.

Brink Helsinki Oy. Cited 30.7.2013. Available at:

http://www.brinkhelsinki.com/visual-storytelling/making-stainless-steel-eight-minutes.

APPENDICES 1-10

Appendix 1. Particle size distribution of CRK dust based on particle volume.

LS Particle Size Analyzer

18 May 2010 11:21

Beckman Coulter LS 13 320

File name:	C:\LS13320\samples\PYOMET\Mikko_A\2010-05-18\CRK Karkea A.$av
	CRK Karkea A.$av
File ID:	ULM
Sample ID:	CRK Karkea A
Comment 2:	1,00g disp. Na4O7P2 0,3% laim.250ml, US 5min, laim.500ml, pip.5ml
Optical model:	Fraunhofer.rfd PIDS included

Volume Statistics (Arithmetic) CRK Karkea A.$av

Calculations from 0.040 µm to 2000 µm

Volume:	100%		
Mean:	2.206 µm	S.D.:	4.226 µm
Median:	0.352 µm	Variance:	17.86 µm^2
Mean/Median ratio:	6.261	C.V.:	192%
Mode:	0.247 µm	Skewness:	2.490 Right skewed
		Kurtosis:	5.242 Leptokurtic

<10%	<25%	<50%	<75%	<90%
0.114 µm	0.181 µm	0.352 µm	1.743 µm	7.393 µm

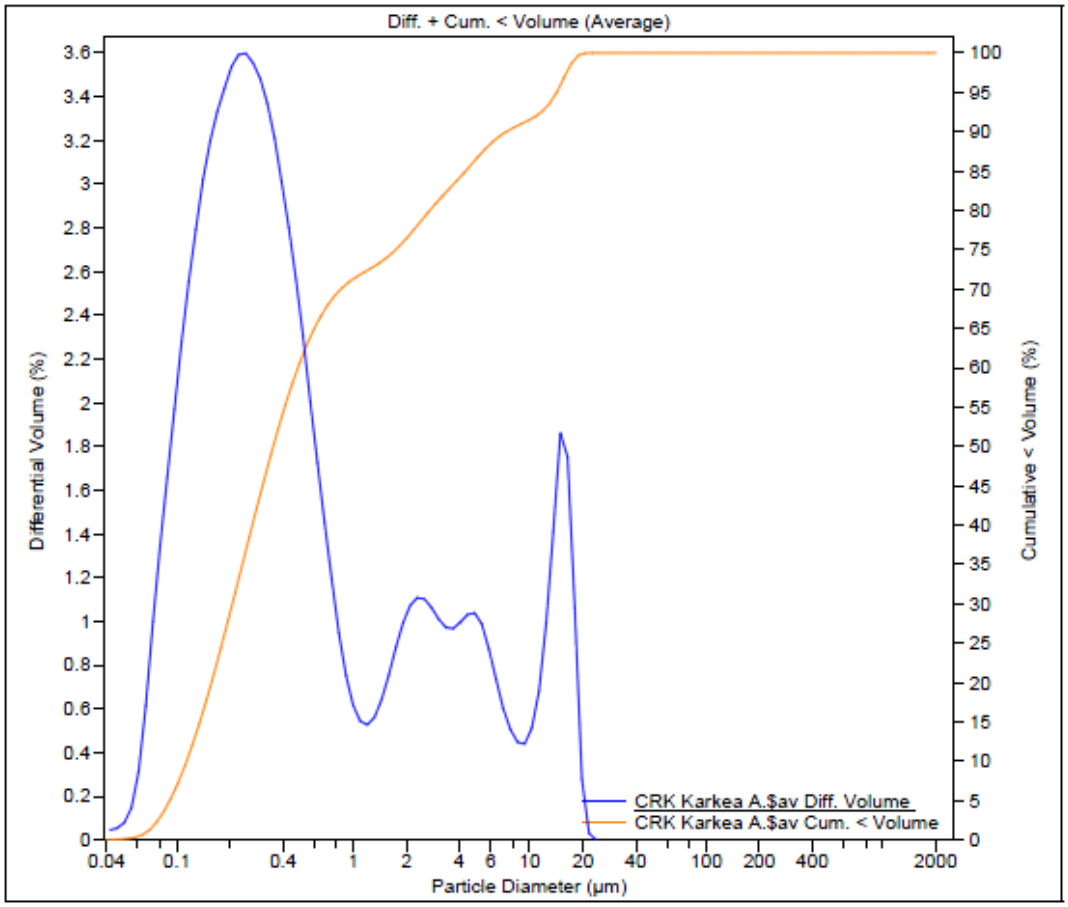

Appendix 2. Particle size distribution of CRK dust based on particle surface area.

BECKMAN COULTER

LS Particle Size Analyzer

18 May 2010 11:21

Beckman Coulter LS 13 320

File name:	C:\LS13320\samples\PYOMET\Mikko_A\2010-05-18\CRK Karkea A.$av
	CRK Karkea A.$av
File ID:	ULM
Sample ID:	CRK Karkea A
Comment 2:	1,00g disp. Na4O7P2 0,3% laim.250ml, US 5min, laim.500ml, pip.5ml
Optical model:	Fraunhofer.rfd PIDS included

Surface Area Statistics (Arithmetic) CRK Karkea A.$av

Calculations from 0.040 µm to 2000 µm

Surface Area:	100%		
Mean:	0.269 µm	S.D.:	0.722 µm
Median:	0.154 µm	Variance:	0.521 µm^2
Mean/Median ratio:	1.744	C.V.:	268%
Mode:	0.117 µm	Skewness:	15.08 Right skewed
		Kurtosis:	287.7 Leptokurtic

<10%	<25%	<50%	<75%	<90%
0.078 µm	0.103 µm	0.154 µm	0.251 µm	0.410 µm

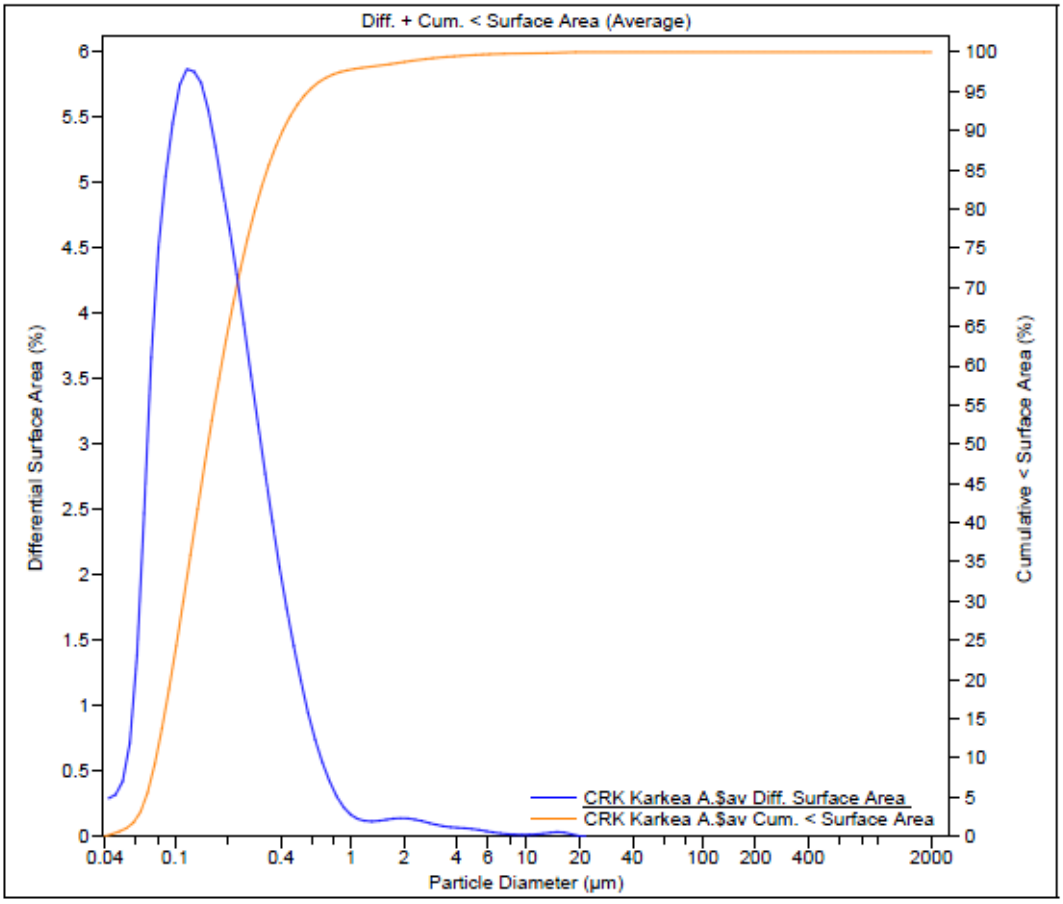

Appendix 3. Particle size distribution of VKU1 dust based on particle volume.

BECKMAN COULTER

LS Particle Size Analyzer

18 May 2010 11:32

Beckman Coulter LS 13 320

File name:	C:\LS13320\samples\PYOMET\Mikko_A\2010-05-18\VKU 1 A.$av
	VKU 1 A.$av
File ID:	ULM
Sample ID:	VKU 1 A
Comment 2:	1,00g disp. Na4O7P2 0,3% laim.250ml, US 5min, laim.500ml, pip. 2ml
Optical model:	Fraunhofer.rfd PIDS included

Volume Statistics (Arithmetic) VKU 1 A.$av

Calculations from 0.040 µm to 2000 µm

Volume:	100%		
Mean:	0.399 µm	S.D.:	0.476 µm
Median:	0.225 µm	Variance:	0.226 µm^2
Mean/Median ratio:	1.772	C.V.:	119%
Mode:	0.205 µm	Skewness:	2.395 Right skewed
		Kurtosis:	5.070 Leptokurtic

<10%	<25%	<50%	<75%	<90%
0.097 µm	0.139 µm	0.225 µm	0.388 µm	1.166 µm

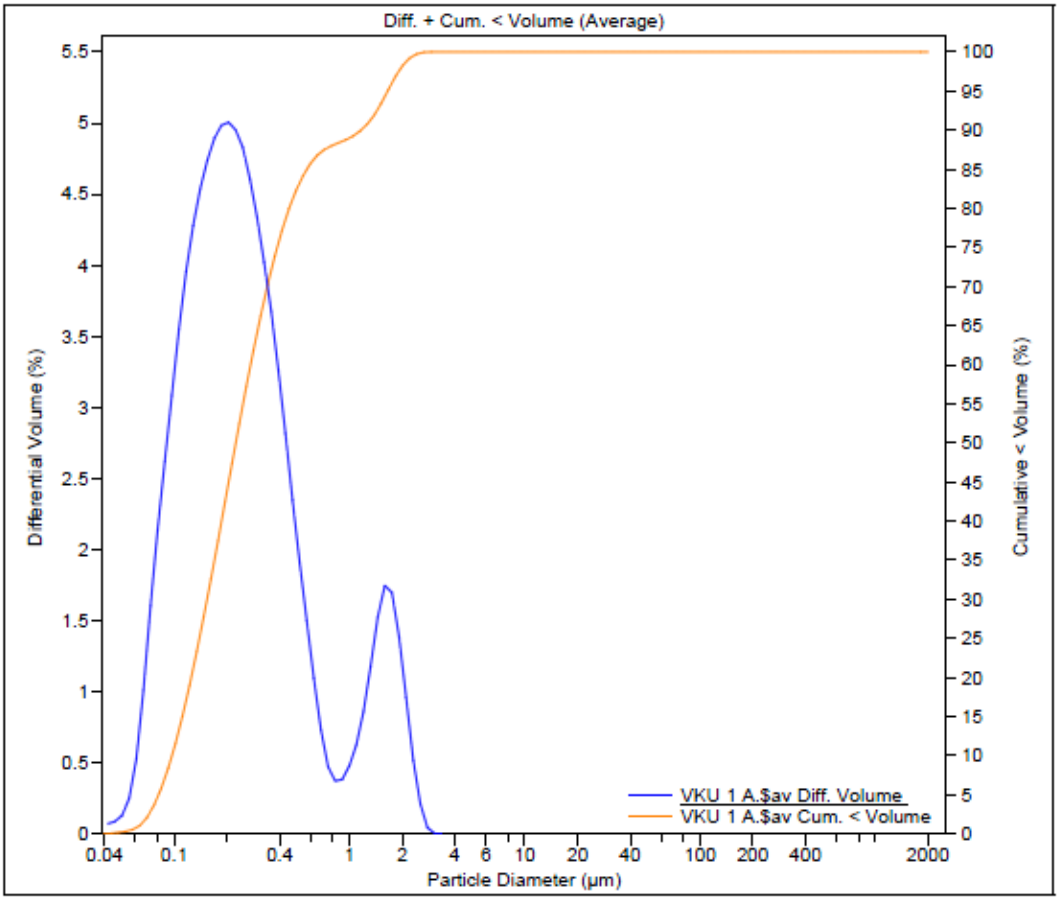

Appendix 4. Particle size distribution of VKU1 dust based on particle surface area.

BECKMAN COULTER

LS Particle Size Analyzer

18 May 2010 11:32

Beckman Coulter LS 13 320

File name:	C:\LS13320\samples\PYOMET\Mikko_A\2010-05-18\VKU 1 A.$av
	VKU 1 A.$av
File ID:	ULM
Sample ID:	VKU 1 A
Comment 2:	1,00g disp. Na4O7P2 0,3% laim.250ml, US 5min, laim.500ml, pip. 2ml
Optical model:	Fraunhofer.rfd PIDS included

Surface Area Statistics (Arithmetic) VKU 1 A.$av

Calculations from 0.040 µm to 2000 µm

Surface Area:	100%		
Mean:	0.192 µm	S.D.:	0.199 µm
Median:	0.141 µm	Variance:	0.040 µm^2
Mean/Median ratio:	1.362	C.V.:	104%
Mode:	0.117 µm	Skewness:	5.564 Right skewed
		Kurtosis:	41.20 Leptokurtic

<10%	<25%	<50%	<75%	<90%
0.076 µm	0.098 µm	0.141 µm	0.217 µm	0.331 µm

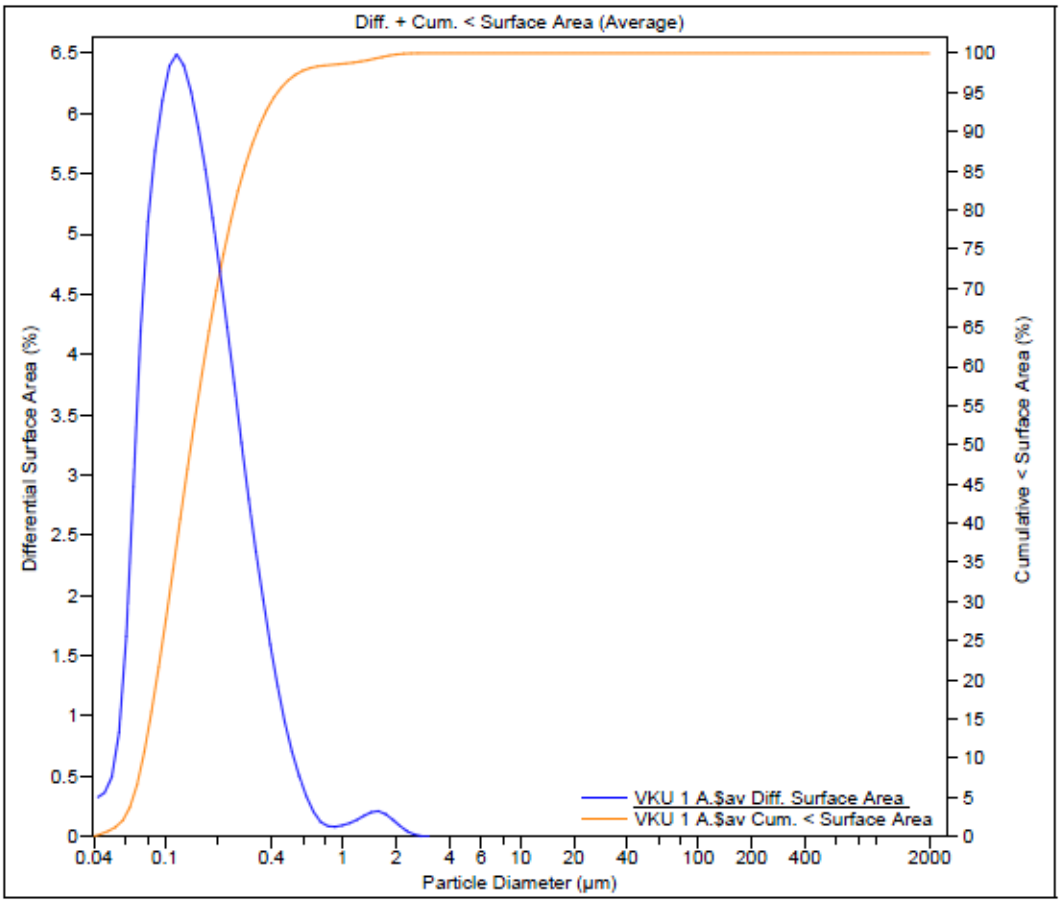

Appendix . Particle size distribution of VKU2 dust based on particle volume.

BECKMAN COULTER

LS Particle Size Analyzer

18 May 2010 11:38

Beckman Coulter LS 13 320

File name:	C:\LS13320\samples\PYOMET\Mikko_A\2010-05-18\VKU 2 Kontti A.$av
	VKU 2 Kontti A.$av
File ID:	ULM
Sample ID:	VKU 2 Kontti A
Comment 2:	1,00g disp Na4O7P2 0,3% 250ml, US 5min, laim.500ml, pip.2ml
Optical model:	Fraunhofer.rfd PIDS included

Volume Statistics (Arithmetic) VKU 2 Kontti A.$av

Calculations from 0.040 µm to 2000 µm

Volume:	100%		
Mean:	0.679 µm	S.D.:	1.074 µm
Median:	0.289 µm	Variance:	1.154 µm^2
Mean/Median ratio:	2.347	C.V.:	158%
Mode:	0.225 µm	Skewness:	3.352 Right skewed
		Kurtosis:	12.18 Leptokurtic

<10%	<25%	<50%	<75%	<90%
0.106 µm	0.162 µm	0.289 µm	0.615 µm	1.705 µm

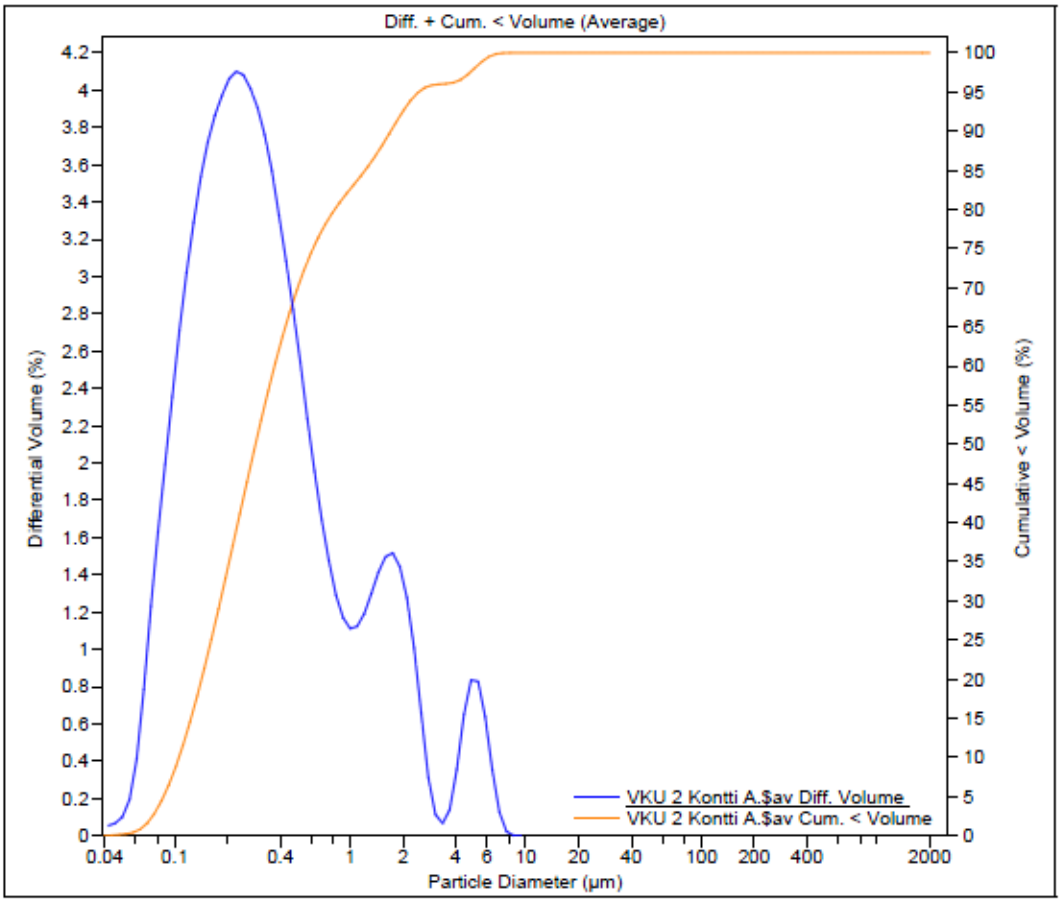

Appendix 6. Particle size distribution of VKU2 dust based on particle surface area.

BECKMAN COULTER

LS Particle Size Analyzer

18 May 2010 11:39

Beckman Coulter LS 13 320

File name:	C:\LS13320\samples\PYOMET\Mikko_A\2010-05-18\VKU 2 Kontti A.$av
	VKU 2 Kontti A.$av
File ID:	ULM
Sample ID:	VKU 2 Kontti A
Comment 2:	1,00g disp Na4O7P2 0,3% 250ml, US 5min, laim.500ml, pip.2ml
Optical model:	Fraunhofer.rfd PIDS included

Surface Area Statistics (Arithmetic) VKU 2 Kontti A.$av

Calculations from 0.040 µm to 2000 µm

Surface Area:	100%		
Mean:	0.230 µm	S.D.:	0.321 µm
Median:	0.151 µm	Variance:	0.103 µm^2
Mean/Median ratio:	1.524	C.V.:	140%
Mode:	0.117 µm	Skewness:	8.676 Right skewed
		Kurtosis:	115.9 Leptokurtic

<10%	<25%	<50%	<75%	<90%
0.077 µm	0.101 µm	0.151 µm	0.246 µm	0.406 µm

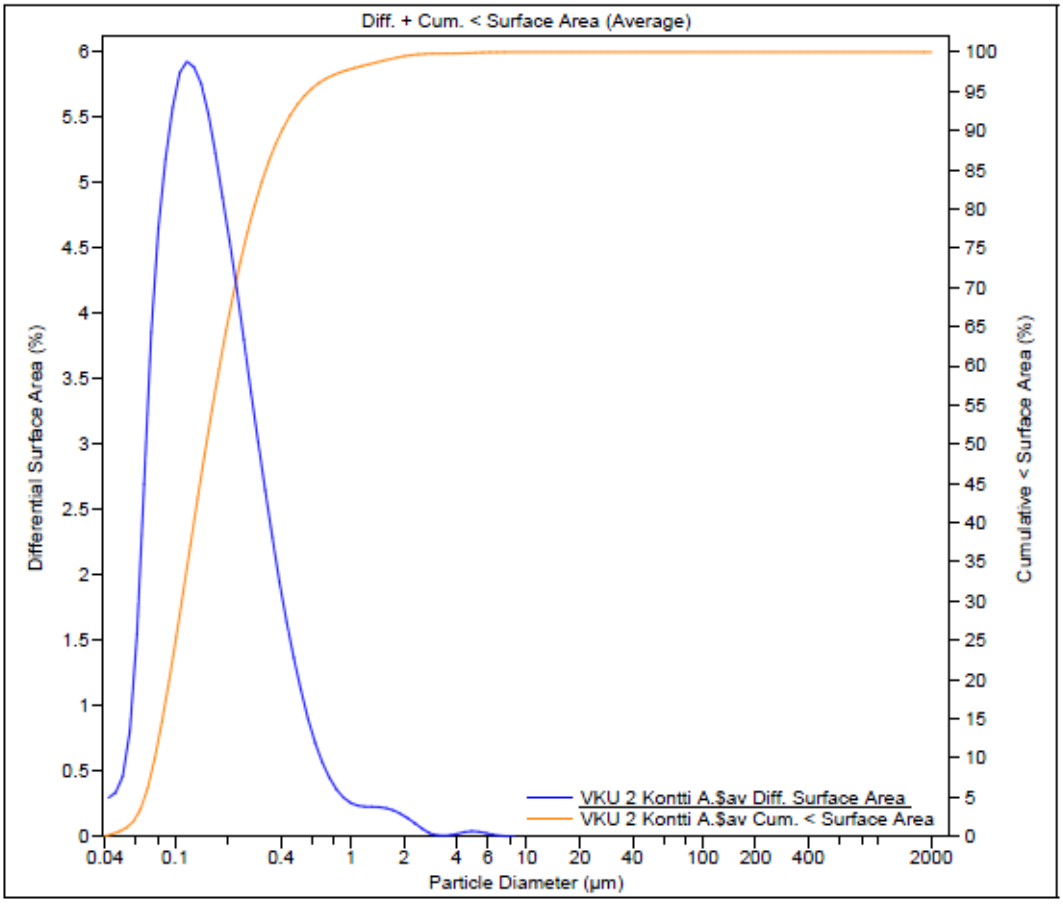

Appendix 7. Particle size distribution of AOD1 dust based on particle volume.

BECKMAN COULTER

LS Particle Size Analyzer

18 May 2010 11:04

Beckman Coulter LS 13 320

File name:	C:\LS13320\samples\PYOMET\Mikko_A\2010-05-18\AOD 1 Kontti A.$av
	AOD 1 Kontti A.$av
File ID:	ULM
Sample ID:	AOD 1 Kontti A
Comment 2:	1,00g disp. Na4O7P2 0,3% laim.250ml, US 5min, laim.500ml, pip. 1ml
Optical model:	Fraunhofer.rfd PIDS included

Volume Statistics (Arithmetic) AOD 1 Kontti A.$av

Calculations from 0.040 µm to 2000 µm

Volume:	100%		
Mean:	0.432 µm	S.D.:	0.462 µm
Median:	0.247 µm	Variance:	0.214 µm^2
Mean/Median ratio:	1.745	C.V.:	107%
Mode:	0.205 µm	Skewness:	1.958 Right skewed
		Kurtosis:	3.096 Leptokurtic

<10%	<25%	<50%	<75%	<90%
0.101 µm	0.147 µm	0.247 µm	0.468 µm	1.215 µm

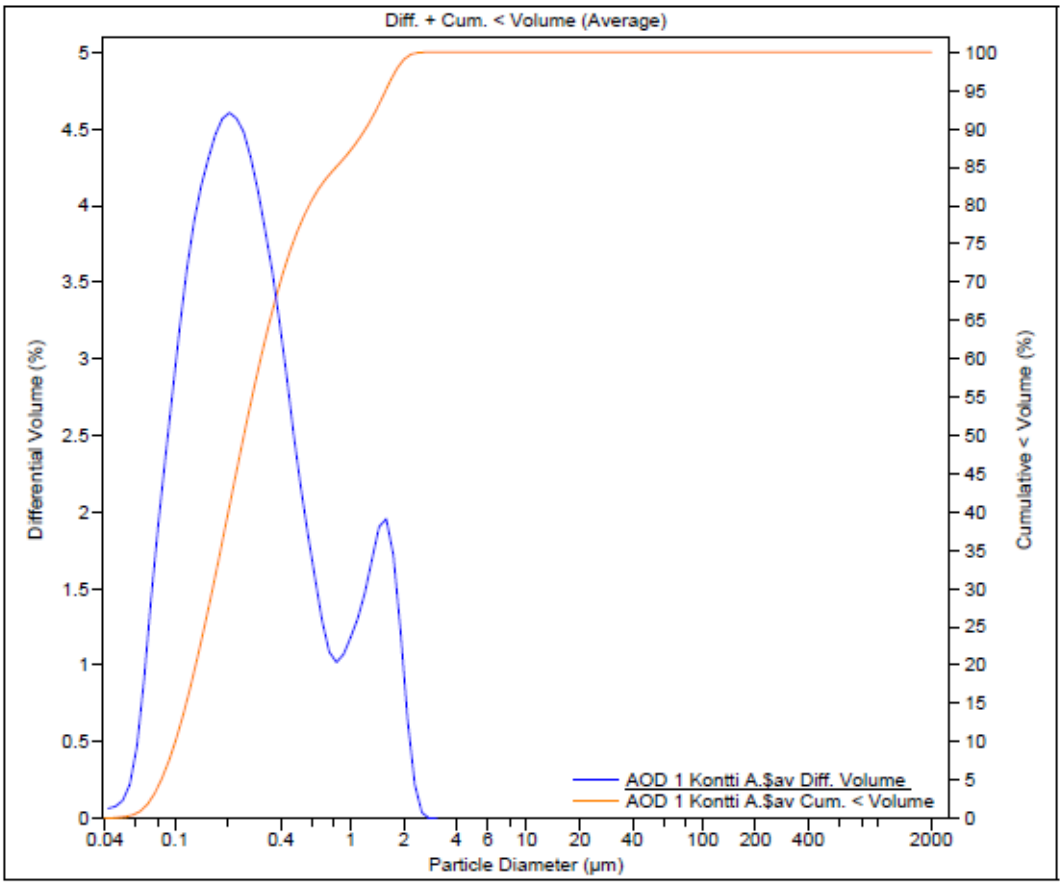

Appendix 8. Particle size distribution of AOD1 dust based on particle surface area.

BECKMAN COULTER

LS Particle Size Analyzer

18 May 2010 11:05

Beckman Coulter LS 13 320

File name:	C:\LS13320\samples\PYOMET\Mikko_A\2010-05-18\AOD 1 Kontti A.$av
	AOD 1 Kontti A.$av
File ID:	ULM
Sample ID:	AOD 1 Kontti A
Comment 2:	1,00g disp. Na4O7P2 0,3% laim.250ml, US 5min, laim.500ml, pip. 1ml
Optical model:	Fraunhofer.rfd PIDS included

Surface Area Statistics (Arithmetic) AOD 1 Kontti A.$av

Calculations from 0.040 µm to 2000 µm

Surface Area:	100%		
Mean:	0.206 µm	S.D.:	0.216 µm
Median:	0.145 µm	Variance:	0.046 µm^2
Mean/Median ratio:	1.422	C.V.:	105%
Mode:	0.117 µm	Skewness:	4.481 Right skewed
		Kurtosis:	26.04 Leptokurtic

<10%	<25%	<50%	<75%	<90%
0.076 µm	0.099 µm	0.145 µm	0.228 µm	0.364 µm

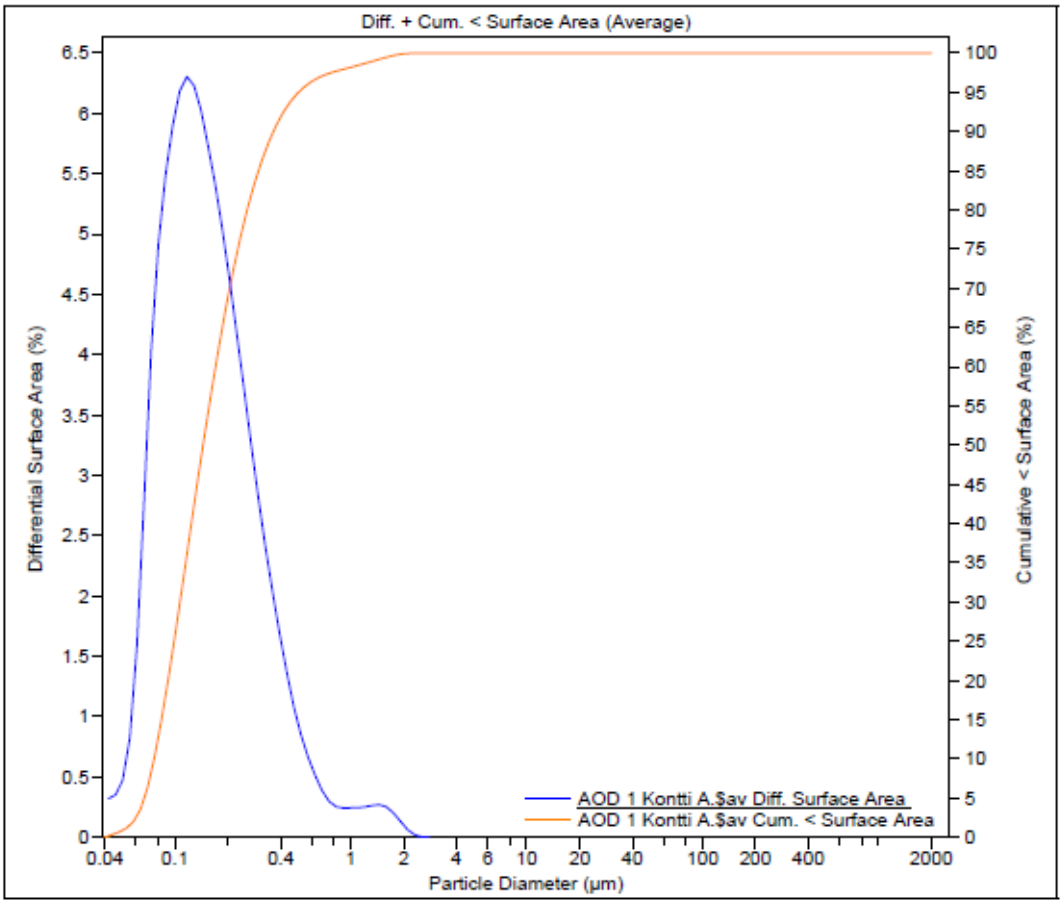

Appendix 9. Particle size distribution of AOD2 dust based on particle volume.

BECKMAN COULTER

LS Particle Size Analyzer

18 May 2010 11:15

Beckman Coulter LS 13 320

File name:	C:\LS13320\samples\PYOMET\Mikko_A\2010-05-18\AOD 2 Kontti A.$av
	AOD 2 Kontti A.$av
File ID:	ULM
Sample ID:	AOD 2 Kontti A
Comment 2:	1,00g disp. Na4O7P2 0,3% laim.250ml, US 5min, laim.500ml, pip. 1,5ml
Optical model:	Fraunhofer.rfd PIDS included

Volume Statistics (Arithmetic) AOD 2 Kontti A.$av

Calculations from 0.040 µm to 2000 µm

Volume:	100%		
Mean:	1.115 µm	S.D.:	2.007 µm
Median:	0.427 µm	Variance:	4.028 µm^2
Mean/Median ratio:	2.611	C.V.:	180%
Mode:	0.225 µm	Skewness:	4.459 Right skewed
		Kurtosis:	22.47 Leptokurtic

<10%	<25%	<50%	<75%	<90%
0.116 µm	0.193 µm	0.427 µm	1.347 µm	2.201 µm

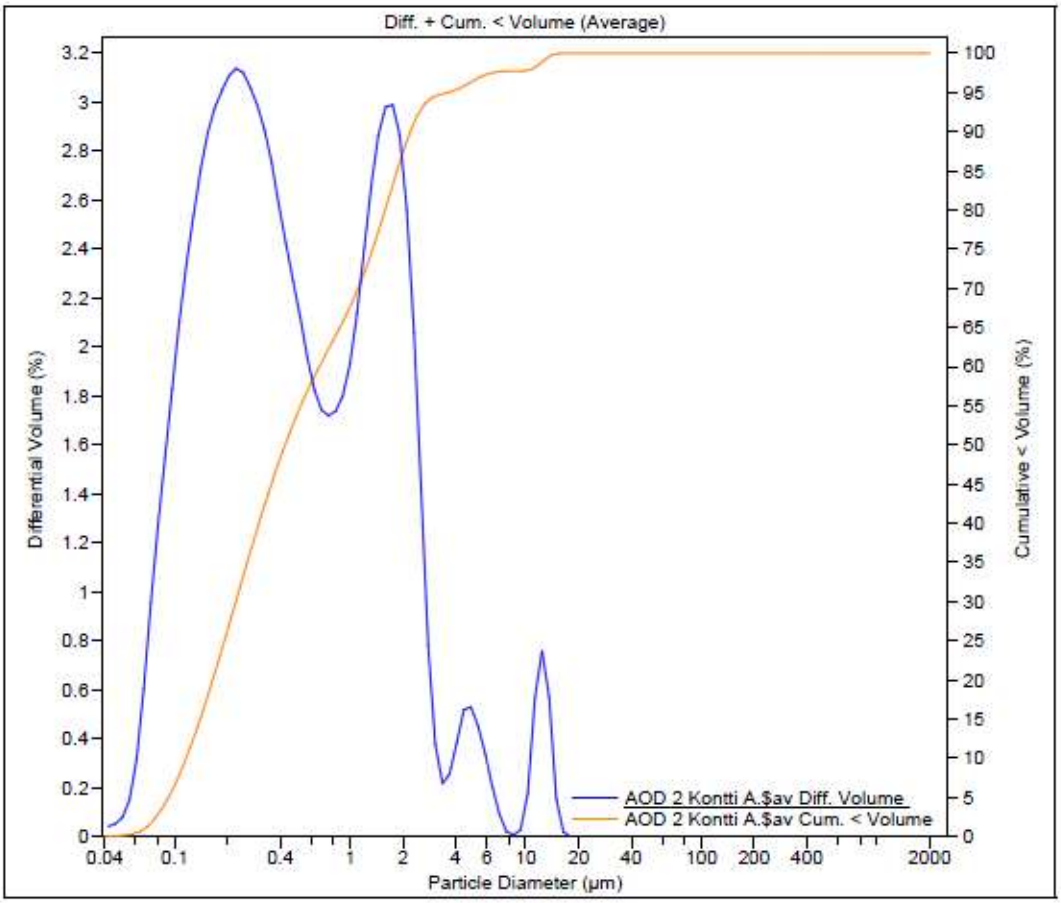

Appendix 10. Particle size distribution of AOD2 dust based on particle surface area.

BECKMAN COULTER

LS Particle Size Analyzer

18 May 2010 11:15

Beckman Coulter LS 13 320

File name:	C:\LS13320\samples\PYOMET\Mikko_A\2010-05-18\AOD 2 Kontti A.$av
	AOD 2 Kontti A.$av
File ID:	ULM
Sample ID:	AOD 2 Kontti A
Comment 2:	1,00g disp. Na4O7P2 0,3% laim.250ml, US 5min, laim.500ml, pip. 1,5ml
Optical model:	Fraunhofer.rfd PIDS included

Surface Area Statistics (Arithmetic) AOD 2 Kontti A.$av

Calculations from 0.040 µm to 2000 µm

Surface Area:	100%		
Mean:	0.284 µm	S.D.:	0.486 µm
Median:	0.156 µm	Variance:	0.236 µm^2
Mean/Median ratio:	1.817	C.V.:	171%
Mode:	0.117 µm	Skewness:	11.10 Right skewed
		Kurtosis:	228.4 Leptokurtic

<10%	<25%	<50%	<75%	<90%
0.078 µm	0.103 µm	0.156 µm	0.269 µm	0.531 µm